HHS Public Access

Author manuscript

J Comp Neurol. Author manuscript; available in PMC 2015 September 28.

Published in final edited form as:

J Comp Neurol. 2013 June 1; 521(8): 1743–1759. doi:10.1002/cne.23254.

Muscarinic Cholinergic Receptor M1 in the Rat Basolateral Amygdala: Ultrastructural Localization and Synaptic Relationships to Cholinergic Axons

Jay F. Muller, **Franco Mascagni**, **Violeta Zaric**, and **Alexander J. McDonald**[*]

Department of Pharmacology, Physiology and Neuroscience, University of South Carolina School of Medicine, Columbia, SC 29208

Abstract

Muscarinic neurotransmission in the anterior basolateral amygdalar nucleus (BLa) mediated by the M1 receptor (M1R) is critical for memory consolidation. Although knowledge of the subcellular localization of M1R in the BLa would contribute to an understanding of cholinergic mechanisms involved in mnemonic function, there have been no ultrastructural studies of this receptor in the BLa. In the present investigation immunocytochemistry at the electron microscopic level was used to determine which structures in the BLa express M1R. The innervation of these structures by cholinergic axons expressing the vesicular acetylcholine transporter (VAChT) was also studied. All perikarya of pyramidal neurons were labeled, and about 90% of dendritic shafts and 60% of dendritic spines were M1R+. Some dendrites had spines suggesting that they belonged to pyramidal cells, whereas others had morphological features typical of interneurons. M1R immunoreactivity (M1R-ir) was also seen in axon terminals, most of which formed asymmetrical synapses. The main targets of M1R+ terminals forming asymmetrical synapses were dendritic spines, most of which were M1R+. The main targets of M1R+ terminals forming symmetrical synapses were M1R+ perikarya and dendritic shafts. About three-quarters of VAChT+ cholinergic terminals formed synapses; the main postsynaptic targets were M1R+ dendritic shafts and spines. In some cases M1R-ir was seen near the postsynaptic membrane of these processes, but in other cases it was found outside of the active zone of VAChT+ synapses. These findings suggest that M1R mechanisms in the BLa are complex, involving both postsynaptic effects as well as regulating release of neurotransmitters from presynaptic terminals.

Keywords

vesicular acetylcholine transporter; immunocytochemistry; electron microscopy; acetylcholine; postsynaptic; presynaptic

[*]**Correspondence to:** Alexander J. McDonald, Ph.D. Department of Pharmacology, Physiology and Neuroscience, University of South Carolina School of Medicine, Columbia, SC 29208, Telephone: 803-216-3511 Fax: 803-216-3524, alexander.mcdonald@uscmed.sc.edu.

Conflict of interest statement: None of the authors have a conflict of interest.

INTRODUCTION

The basolateral nuclear complex of the amygdala (BLC) has some of the highest levels of choline acetyltransferase (ChAT; the synthetic enzyme for acetylcholine) and acetylcholinesterase (the catabolic enzyme for acetylcholine) in the entire brain (Ben-Ari et al., 1977; Girgis, 1980; Svendsen and Bird, 1985; Hellendall et al., 1986; Amaral and Bassett, 1989). Studies combining ChAT immunohistochemistry with retrograde tract tracing have demonstrated that the cholinergic basal forebrain, especially the Ch4 group in the substantia innominata, is the main source of these robust cholinergic inputs to the amygdala in both rodents (Mesulam et al., 1983a; Woolf et al., 1984, Carlsen et al., 1985; Zaborsky et al., 1986; Rao et al., 1987) and primates (Mesulam et al., 1983b; Koliatsos et al., 1988; Kordower et al., 1989). Recent studies have shown that acetylcholine is critical for mnemonic functions performed by the BLC (McGaugh, 2004). Although cholinergic inputs to the BLC are associated with both nicotinic and muscarinic receptors, most studies of memory consolidation utilized muscarinic antagonists (Power et al., 2003a). Posttraining infusions of muscarinic cholinergic antagonists into the BLC, or lesions of the portions of the basal forebrain cholinergic system projecting to the amygdala, produce impairments in several types of emotional/motivational learning including inhibitory avoidance, contextual fear conditioning, food reward magnitude learning, conditioned place preference, and drug-stimulus learning (Power et al., 2003a). In fact, it has been suggested that the degeneration of the cholinergic projections to the BLC in Alzheimer's disease may be at least as important for the memory disturbances seen in this disorder as the cholinergic projections to the cortex (Kordower et al., 1989; Power et al., 2003a).

Power and colleagues demonstrated that activation of both M1 and M2 muscarinic receptors in the anterior basolateral nucleus (BLa) of the rat BLC is needed for memory consolidation functions performed by this brain region (Power et al., 2003b). Although knowledge of the cellular and subcellular localization of these receptors in the BLa is critical for understanding the actions of acetylcholine involved in consolidation of memory, previous receptor binding autoradiographic studies and film-based in situ hybridization studies lacked the resolution necessary to identify which neurons and synapses in the BLa express different muscarinic receptor subtypes. Likewise, electrophysiological investigations of neuronal responses to muscarinic drugs have been hampered by the lack of receptor subtype specific agonists and antagonists (Ehlert et al., 1995). However, the development of antibodies to specific muscarinic receptor subtypes has permitted immunohistochemical localization of these receptor proteins at the light and electron microscopic levels (Levey et al., 1991; Mrzljak et al., 1993, Rouse et al., 1998; Disney et al., 2006). Pharmacological studies have found at least 4 muscarinic receptor subtypes (designated by upper case letters as M1-M4), whereas molecular biological techniques have identified 5 distinct subtypes (designated by lower case letters as m1-m5) (Ehlert et al., 1995). In the present study we performed an ultrastructural analysis using an m1 receptor subtype specific antibody. For convenience, this receptor will be abbreviated "M1R", with the understanding that it is actually the m1 molecular subtype that was localized.

The initial immunohistochemical study of the rat forebrain revealed that the M1R was the predominant muscarinic receptor subtype in the amygdala, but no details of the nuclear or

neuronal localization of these receptors was provided (Levey et al., 1991). We recently examined the distribution of M1R immunoreactivity (M1R-ir) in the amygdala in more detail and observed that the highest levels were in the BLa (McDonald and Mascagni, 2010). This study also revealed that there was robust M1R immunoreactivity in the somata of pyramidal neurons, the principal neurons of the BLa, and little or no M1R-ir in the somata of most interneurons. The neuropil of the BLa had very high levels of punctate M1R-ir, but the nature of these labeled structures could not be resolved in this light microscopic study. The present investigation is the first electron microscopic investigation of the ultrastructural localization of M1R in the BLa. In addition, the cholinergic innervation of M1R-ir structures was investigated using immunocytochemistry for the vesicular acetylcholine transporter protein (VAChT) to identify cholinergic axons.

MATERIALS AND METHODS

Light microscopic immunohistochemistry

Slides from a prior light and confocal microscopic study of M1R in the BLa (McDonald and Mascagni, 2010) were used to illustrate the distribution of this receptor in the perikarya and neuropil of the BLa at the light microscopic level (see Fig. 1 of the present study). Localization of the M1R muscarinic cholinergic receptor was performed using the avidin-biotin immunoperoxidase (ABC) technique. Nickel-enhanced DAB (3, 3'-diaminobenzidine-4HCl, Sigma Chemical Co.) was used as a chromogen to generate a black reaction product (Hancock, 1986). In other rats localization of M1R was performed using immunofluorescence techniques (see McDonald and Mascagni, 2010 for methodological details of both techniques). The same M1R antibody used in these previous light microscopic studies was also used in the present electron microscopic study.

Tissue preparation for electron microscopy

All experiments were performed in male Sprague-Dawley rats (250–350 g; Harlan) and were carried out in accordance with the principles of laboratory animal care (NIH publication no. 86–23, revised 1985). All procedures were approved by the University of South Carolina Institutional Animal Care and Use Committee. Rats were anesthetized with chloral hydrate (350 mg/kg), and perfused intracardially with phosphate buffered saline (PBS; pH 7.4) containing .5% sodium nitrite (50 ml) followed by an acrolein/paraformaldehyde mixture (2.0% paraformaldehyde-3.75% acrolein in phosphate buffer (PB) for 1 minute, followed by 2.0% paraformaldehyde in PB for 30 minutes). Following removal, brains were postfixed in 2.0% paraformaldehyde for 1 hour and sectioned on a vibratome in the coronal plane at 60 μm. Sections were rinsed in 1.0% borohydride in PB for 30 minutes and then rinsed thoroughly in several changes of PB for 1 hour. Sections were then cryoprotected in 30% sucrose in PB for 3 hr, followed by three cycles of freeze-thaw over liquid nitrogen in order to increase antibody penetration. They were then processed for immunocytochemistry in the wells of tissue culture plates.

Single-labeling electron microscopic immunocytochemistry for M1R

Single-label electron microscopic immunocytochemistry using a nickel-intensified DAB immunoperoxidase method was performed in 5 rats to analyze the ultrastructural localization

of M1R in the anterior subdivision of the basolateral nucleus (BLa; bregma levels -2.1 through -2.6; Paxinos and Watson, 1997). The BLa was chosen for study because it receives the densest cholinergic innervation in the amygdala, and since M1R in the BLa is known to be critical for memory consolidation of emotionally arousing experiences (McGaugh, 2004). Sections through the BLa were incubated in a rabbit polyclonal antibody to M1R (1:250–400; Sigma Chemical Company, St. Louis, MO) for 36 hrs at 4° C in PBS containing 1% normal donkey serum (NDS) and 2% bovine serum albumin (BSA), and then processed using a biotinylated donkey anti-rabbit secondary antibody (1:200; Jackson ImmunoResearch Laboratories) and a Vectastain Standard ABC kit (Vector Laboratories, Burlingame, CA) with nickel-enhanced DAB (3, 3'-diaminobenzidine-4HCl, Sigma) as a chromogen to generate a black reaction product (Hancock, 1986). Sections were then postfixed in 2% osmium tetroxide in 0.16 M sodium cacodylate buffer (pH 7.4) for 1 hr, dehydrated in graded ethanols and acetone, and flat embedded in Polybed 812 (Polysciences, Warrington, PA) in slide molds between sheets of Aclar (Ted Pella, Redding, CA). Silver thin-sections were collected on formvar-coated slot grids, stained with uranyl acetate and lead citrate, and examined with a JEOL-200CX electron microscope. Micrographs were taken with an AMT XR40 digital camera system (Advanced Microscopy Techniques, Danvers, MA). For publication, figures were then assembled, labeled and their components' tonal ranges adjusted and matched using Adobe Photoshop 6.0.

Electron microscopic double-label immunocytochemistry

Electron microscopic immunocytochemistry using a sequential dual-labeling immunoperoxidase method (Muller et al., 2006) was utilized in 6 rats to examine the synaptic relationships of cholinergic axon terminals to M1R+ structures. A goat polyclonal antibody to the vesicular acetylcholine transporter (VAChT; ImmunoStar, Hudson, WI) was used to label cholinergic axons (Weihe et al., 1996; Gilmor et al., 1996). Sections were incubated for 36 hrs at 4° C in the rabbit M1R antibody (1:100) diluted in PBS containing 3% NDS and 1% BSA, and processed using a biotinylated donkey anti-rabbit secondary antibody (1:200; Jackson ImmunoResearch Laboratories) for 1 hr and a Vectastain Elite ABC kit (Vector Laboratories). M1R immunoreactivity was then visualized using a Vector VIP (Very Intense Purple) peroxidase substrate kit (V-VIP; Vector Laboratories). This procedure yields a reaction product that appears purple in the light microscope, and granular or particulate in the electron microscope (Smiley et al., 1997; Van Haeften and Wouterlood, 2000; Muller et al., 2006). After rinsing, sections were incubated in an avidin/biotin blocking solution (avidin/biotin blocking kit, Vector Laboratories). Sections were then incubated for 36 hrs at 4°C in a goat VAChT antibody (1:4,000) in PBS containing 3% NDS and 1% BSA, and processed using a biotinylated donkey anti-goat secondary antibody (1:300; Jackson ImmunoResearch Laboratories) for 1 hr and a Vectastain Standard ABC kit (Vector Laboratories) with non-intensified DAB as the chromogen to produce a brown reaction product. Sections were then processed for electron microscopy as described above. Light and electron microscopic examination of sections processed using this dual-labeling DAB/V-VIP immunoperoxidase method, but with one of the two primary antibodies omitted, produced no reaction product for the chromogen associated with the omitted antibody.

Analysis

Profiles were identified as perikarya, axon initial segments, large-caliber dendrites (>1 μm), small-caliber dendrites (<1 μm), dendritic spines, and axon terminals using established morphological criteria (Peters et al., 1991). For both single and double-label preparations, one or two vibratome sections were chosen from each brain that was selected for quantitative analysis. Serial sections were analyzed and often followed on consecutive grids. Serial sections were helpful for verifying label in small and lightly immunoreactive structures, and determining the synaptic nature of contacts. In the single-labeled nickel-intensified DAB material, M1R-positive and M1R-negative dendrites and spines were tallied and pooled from the two brains judged to have the best ultrastructural preservation and immunohistochemistry for M1R. For each vibratome section, areas that exhibited the best morphology and immunohistochemistry were chosen within a single thin section, and then all M1R-positive and M1R-negative dendrites and spines were counted in that area, and followed serially only to ascertain identification and label. This analysis provided an estimate of the percentage of dendrites and spines that were M1R+.

M1R+ axon terminals forming asymmetrical (presumptive excitatory) synapses or symmetrical (predominantly inhibitory) synapses were counted in both the single-labeled nickel-intensified DAB material, as well as in the M1R/VAChT dual-labeled material (in which M1R was visualized using the V-VIP chromogen), and the postsynaptic targets of these terminals, as well as whether they were M1R-positive or negative, were noted. In both preparations, the distribution of M1R+ terminals was not uniform; some regions had few M1R+ terminals and other regions had several M1R+ terminals in close proximity. Therefore in order to get a general survey of M1R+ terminals and their targets, areas for analysis were selected from a variety of neuropilar compartments (e.g., different areas exhibiting a predominance of perikarya, small-caliber dendrites or large-caliber dendrites). For both techniques, counts were tallied and pooled from the two brains judged to have the best ultrastructural preservation and immunohistochemistry for M1R. Synapses were identified using standard criteria: 1) parallel presynaptic and postsynaptic membranes exhibiting membrane thickenings, 2) a synaptic cleft containing dense material, and 3) clustered synaptic vesicles associated with the presynaptic membrane (Peters et al., 1991). Asymmetrical and symmetrical synapses were identified based on the presence or absence, respectively, of a prominent postsynaptic density and on the relative widths of their synaptic clefts. Whereas synaptic clefts of asymmetrical synapses are typically 20 nm wide, symmetrical synapses have a much narrower synaptic cleft that is only about 12 nm wide (Peters et al., 1991).

The cholinergic innervation of M1R-ir structures was investigated in the M1R/VAChT dual-labeled material. Data analysis focused on the synaptic contacts formed by VAChT+ axon terminals with M1R-positive and M1R-negative structures in the two brains judged to have the best ultrastructural preservation and immunohistochemistry for VAChT and M1R. VAChT+ axon terminals were followed through serial sections and the postsynaptic targets of these terminals, as well as whether they were M1R-positive or negative, were noted.

Antibody Specifity

Table 1 provides a list of primary antibodies used in this study. The m1R antibody (catalog # M-9808; Sigma Chemical Co) was raised in rabbit to a highly purified GST fusion protein of a part of the third intracellular loop of the human m1 receptor corresponding to amino acids 227–353. This part of the third intracellular loop shows virtually no sequence homology with other muscarinic receptor subtypes, but is homologous between species (Bonner et al., 1987). The specificity of this antibody for the m1R has been previously established (Levey et al., 1991). Immunoblotting demonstrated a protein band that was distinct from other muscarinic receptor subtypes. Immunoprecipitation experiments demonstrated that this antiserum only bound the m1R receptor subtype. Preadsorption of the antiserum with the third intracellular loop fusion protein blocked antibody binding.

The VAChT antibody (catalog# 24286, ImmunoStar, Hudson, WI) was raised in goat using a synthetic carboxy-terminal 20-amino-acid sequence (511–530) from the cloned rat VAChT as an immunogen, and has previously been characterized (Arvidsson et al., 1997). The antiserum immunohistochemically stains CV-1 cells transfected with rat VAChT cDNA, but not vesicular monoamine transporter-2 (VMAT-2) cDNA (Arvidsson et al., 1997). VAChT immunoreactivity was also seen in cells that are known to express the protein, such as PC12 cells and cultured spinal motoneurons. Preadsorption of the antiserum with the immunizing peptide completely abolished immunostaining (Arvidsson et al., 1997).

RESULTS

Light microscopic examination revealed that M1R-immunoreactivity (M1R-ir) in the amygdala was dense in the basolateral nuclear complex and most robust in the BLa (Fig. 1A). There was strong perikaryal staining as well as significant neuropilar labeling in the BLa (Figs. 1B, C). Virtually all of the perikaryal staining appeared to be confined to pyramidal cells.

Electron microscopic examination of sections stained using nickel-intensified DAB (Ni-DAB) confirmed that M1R-ir was located in perikarya of presumptive pyramidal cells, and also demonstrated that there were a variety of M1R+ structures in the neuropil (Fig. 2). In these preparations, M1R-ir in perikarya was generally diffuse, and found associated with the endoplasmic reticulum and Golgi apparatus, as well as near the plasma membranes (Fig. 2C). Counts of dendritic structures revealed that 94% (46/49) of large-caliber dendrites (> 1 μm), 90% (189/210) of small-caliber dendrites (< 1 μm), and 57% (109/190) of spines were M1R+. The cell types of origin of most of the M1R+ dendrites could not be determined based on their morphology, although the presence of spines on some of the dendrites (Fig. 2A) suggested that they might belong to pyramidal cells. However, a few M1R+ dendritic shafts received multiple asymmetrical synapses typical of BLa interneuronal dendrites (Muller et al., 2011) (Fig. 2B). Much of the DAB reaction product in dendrites and spines was cytoplasmic. In dendrites this label was associated with microtubules and outer mitochondrial membranes, but in many dendrites and spines there was also M1R-ir at or near the plasma membrane as well (Figs. 2, 3). Similar subcellular localization of M1R-ir in perikarya and dendrites was seen in preparations where particulate V-VIP was used as the chromogen (Figs. 4– 9).

Many M1R+ axon terminals were seen in the neuropil in both Ni-DAB (Figs. 2 and 3) and V-VIP preparations (Figs. 4– 6). In sections stained using Ni-DAB as a chromogen, 90% (135/151) of the M1R+ terminals formed asymmetrical synapses, and 10% (15/151) formed symmetrical synapses. In sections stained using V-VIP as a chromogen for visualizing M1R-ir, 79% (124/157) of the M1R+ terminals formed asymmetrical synapses, and 21% (33/157) formed symmetrical synapses (VAChT+ terminals stained with DAB in this V-VIP/DAB dual-labeled material were disregarded in these counts). M1R+ terminals in the Ni-DAB material typically had flocculent staining along the membranes of synaptic vesicles and mitochondria, as well as more concentrated reaction product adjacent to the active zone of the presynaptic membrane (Figs. 2 and 3). Most of the M1R+ terminals in the V-VIP material had concentrated particulate reaction product at or near the active zone of the presynaptic membrane, but occasional non-plasmalemmal-associated particles were also seen (Figs. 4– 6). The postsynaptic targets of M1R+ terminals were fairly similar among the four brains used for quantitation, although the incidence of certain target structures, such as perikarya and large dendrites, varied in the fields surveyed in different brains. As shown in Table 2, combined counts from the Ni-DAB and V-VIP preparations revealed that the postsynaptic targets of M1R+ terminals forming asymmetric synapses were as follows: 1.2% (3/260) were perikarya (all of which were M1R+), 7.3% (19/260) were large-caliber dendrites (all of which were M1R+), 18.1% (47/260) were small-caliber dendrites (93.6% of which were M1R+), and 73.5% (191/260) were spines (88.0% of which were M1R+). As shown in Table 3, the postsynaptic targets of M1R+ terminals forming symmetric synapses in these fields were as follows: 39.6% (19/48) were perikarya or axon initial segments (14 perikarya and 5 axon initial segments [Fig. 5B], all of which were M1R+), 8.3% (4/48) were large-caliber dendrites (all of which were M1R+), 41.7% (20/48) were small-caliber dendrites (all of which were M1R+), and 10.4% (5/48) were spines (60.0% of which were M1R+). Thus, the main targets of M1R+ terminals forming asymmetrical synapses were M1R+ spines, whereas the main targets of M1R+ terminals forming symmetrical synapses were M1R+ perikarya/axon initial segments and small-caliber dendrites.

Some M1R+ terminals forming symmetrical synapses were very large and had numerous synaptic vesicles and mitochondrial profiles, characteristic of the distinctive type 1 axon terminals of GABAergic basal forebrain afferents to the BLa (McDonald et al., 2011). These terminals were seen forming synapses with M1R+ perikarya and dendrites (Figs. 2C, 6; compare to McDonald et al., 2011: Figs. 5– 7).

In tissue dual-labeled for M1R and VAChT (using V-VIP and DAB as chromogens, respectively) a total of 109 VAChT+ cholinergic axon terminals were reconstructed from serial thin sections (n = 4–10 thin sections per terminal). 76% (83/109) of these VAChT+ terminals formed at least one synapse, all of which were symmetrical. Of the 99 synapses formed by these 83 terminals, 3.0% (3/99) were with perikarya (all of which were M1R+), 5.1% (5/99) were with large-caliber dendrites (all of which were M1R+), 41.4% (41/99) were with small-caliber dendrites (all of which were M1R+), and 50.5% (50/99) were with spines (86.0% of which were M1R+) (Table 4). Thus, the main postsynaptic targets of VAChT+ cholinergic terminals in the BLa were M1R+ small caliber dendrites and spines (Figs. 7, 8, 9). M1R+ particulate label was seen along the postsynaptic membrane at some cholinergic synapses (Fig. 7D, 9A), but not others (Fig. 7A, 7B, 8). However, in the latter

instances there was often membrane-associated label along the plasma membrane adjacent to the synapse (e.g., Fig. 7A). Concentrated particulate reaction product similar to that seen along the presynaptic membrane of M1R+ axon terminals was not observed along the postsynaptic membrane associated with VAChT+ terminals.

VAChT+ terminals were often adjacent to non-cholinergic M1R+ terminals, and sometimes both types of terminals synapsed with the same dendritic shaft or spine (Fig. 8). Electron microscopic examination revealed that the density of VAChT+ terminals in the BLa was very high and that it was not uncommon to see several M1R+ terminals within 1–2 μm of VAChT+ terminals (Fig. 9; also see Figure Description for Fig. 6).

DISCUSSION

Pyramidal cells are the main BLa cell type expressing M1R-ir

Previous light microscopic studies had shown that the perikarya of all pyramidal neurons in the BLa were M1R+, and that the neuropil of the BLa exhibited a very high density of small M1R+ structures whose identity could not be determined (McDonald and Mascagni, 2010). Consistent with the latter observation, the present ultrastructural analysis demonstrated that about 90% of dendritic shafts, 60% of dendritic spines, and many axon terminals in the BLa were M1R+. In two cortical areas subjected to similar quantitation of M1R+ structures the percentages were less. Thus, analysis of the outer molecular layer of the rat dentate gyrus using immunoperoxidase techniques revealed that 70% of dendritic shafts, 50% of dendritic spines, and 4% of axon terminals were M1R+ (Rouse et al., 1998). Using the less sensitive immunogold-silver technique, examination of the monkey visual cortex demonstrated that only about one-quarter of dendritic shafts, 9% of dendritic spines, and 4% of axon terminals were M1R+ (Disney et al., 2006). The higher percentages of M1R+ dendrites in the BLa may reflect the very dense cholinergic innervation and the high levels of M1R expression in this nucleus.

The present investigation demonstrated that much of the M1R-ir in the perikarya of pyramidal cells was found in close association with the endoplasmic reticulum and Golgi apparatus, suggesting that it is being packaged for transport to the plasma membrane of the processes of these neurons. Since it is thought that the vast majority of spines seen at the EM level belong to pyramidal cells (see Muller et al., 2006 for a discussion) it is highly likely that almost all of the M1R+ spines, which constituted 57% of all spines, are of pyramidal cell origin. Most of the M1R-ir in dendritic shafts was cytoplasmic, rather than being associated with the plasma membrane, suggesting that it represents M1R that is in the process of being transported to or from more distal dendrites and/or spines.

Although some M1R+ dendritic shafts received multiple asymmetrical synapses typical of BLa interneuronal dendrites (Muller et al., 2011), the cell type of origin of the great majority of M1R+ dendrites could not be determined. The best evidence that the great majority of M1R+ dendritic shafts belong to pyramidal cells comes from comparing the data from the VAChT/M1R dual-labeling studies with data from a previous study of the cholinergic innervation of pyramidal cells (Muller et al., 2011). The data from the VAChT/M1R studies indicate that all of the dendritic shafts targeted by VAChT+ terminals were M1R+ in the

quantitative analysis. In a previous investigation examining VAChT+ terminals that synapse with pyramidal cell dendritic shafts exhibiting immunoreactivity for calcium/calmodulin-dependent protein kinase II (CaMK), a specific marker for BLa pyramidal cells, it was found that 82% of the dendritic shafts that were postsynaptic to VAChT+ terminals were CaMK+ (Muller et al., 2011). Taken together, these data imply that at least three-quarters of the M1R + dendritic shafts seen in the present study belong to pyramidal cells. In addition, some of the M1R+ dendrites were spiny, further suggesting a pyramidal cell origin. Pyramidal cells constitute about 85% of BLa neurons, and their dendritic arborizations are much more complex than those of interneurons (McDonald, 1992b). Therefore, it seems likely that pyramidal cell dendrites may constitute about 90–95% of dendritic profiles seen with the electron microscope. In light of the robust labeling of dendritic shafts of presumptive pyramidal cells, as well as the labeling of presumptive interneuronal dendrites (see below), it is not surprising that 90% of dendritic shafts in the BLa were M1R+ in our study.

M1Rs must be inserted into the plasma membrane to be functional. In sections processed using Ni-DAB as a chromogen, no accumulation of reaction product was observed at the plasma membrane of M1R+ dendrites, but there were accumulations of DAB reaction product at the presynaptic membrane of M1R+ terminals. Similarly, the particulate V-VIP reaction product was usually restricted to this presynaptic location in M1R+ axon terminals, suggesting that these particles are associated with high concentrations of M1R. Likewise, the particulate V-VIP reaction product contacting the plasma membrane of dendritic shafts may reflect membrane-associated receptor. However, future studies using techniques with more precise localization of antigen (e.g., immunogold techniques), will be required to provide a more definitive answer to this question.

The presence of M1R-ir in 60% of dendritic spines suggests that the activity of these spines is regulated via M1Rs. In a previous study in this lab there was evidence that the peroxidase reaction product of CaMK imunohistochemistry in the shafts of pyramidal dendrites did not spread into spines (McDonald et al., 2002). If this is also the case with the M1R imunohistochemistry in the present study, it would imply that M1R-ir in spines is due to localization of M1R in the spine, and not due to spread of reaction product from the attached dendritic shaft. Thus, our spine data suggests that the inputs to a subset of dendritic spines, which are mainly provided by axon terminals forming asymmetrical (excitatory) synapses, may be modulated by acetylcholine via postsynaptic M1Rs.

Since M1R is the main muscarinic receptor subtype in the basolateral amygdala (Buckley et al., 1988; Levey et al., 1991), and most of the M1R-ir is found in pyramidal cells (McDonald and Mascagni, 2010; present study), it seems likely that many of the muscarinic responses observed in pyramidal cells are mediated by this receptor subtype. One of the main effects of muscarinic agonists and/or stimulation of cholinergic afferents to the amygdala is an increase in the excitability of BLa pyramidal cells due to the suppression of several potassium currents, including the muscarine-sensitive M-current (I_M), the voltage-insensitive leak current (I_{Leak}), and the calcium-activated slow afterhyperpolarization current (sI_{AHP}) (Washburn and Moises, 1992, Womble and Moises, 1992, 1993). The finding that the M1R antagonist pirenzepine attenuates the carbacol-induced suppression of the sI_{AHP} in BLa pyramidal cells suggests that this effect is mediated, at least in part, by the

M1R (Washburn and Moises, 1992). In addition, a recent study has demonstrated that activation of muscarinic cholinergic receptors activate small conductance calcium-activated potassium (SK) channels in BLa pyramidal cells following the release of calcium from intracellular stores via activation of the phosphatidylinositol signal transduction pathway (Power and Sah, 2008). Since M1Rs are known to activate the phosphatidylinositol system (Richelson, 1995), these receptors may mediate this response in BLa pyramidal cells.

Interneurons express M1R-ir

In a previous immunofluorescence study employing glutamic acid decarboxylase (GAD) as a marker for GABAergic interneurons in the BLa, it was found that very few GAD+ perikarya had levels of M1R-ir that exceeded that seen in the neuropil, but many had a few particles of M1R-ir (McDonald and Mascagni, 2010). It was suggested that these lightly labeled interneuronal perikarya might express low levels M1R-ir due to the rapid transport of the receptor protein to their processes. Indeed, in the present study some M1R+ dendritic shafts in the BLa received multiple asymmetrical synapses (Fig. 2B) typical of BLa interneuronal dendrites (Muller et al., 2011). Since pyramidal cell somata in the BLa don't receive inputs via asymmetrical synapses (Muller et al., 2006), the three M1R+ perikarya that were postsynaptic to the M1R+ terminals forming asymmetrical synapses (Table 2) probably belong to interneurons. Also many of the M1R+ axon terminals forming symmetrical synaptic contacts with the perikarya and axon initial segments of M1R+ neurons (Table 3), most of which are probably pyramidal cells, may arise from the axons of parvalbumin-containing interneuronal basket cells and chandelier cells (Muller et al., 2006). Previous electron microscopic studies have demonstrated that the somata and dendrites of GABAergic BLa interneurons are innervated by cholinergic inputs (Carlsen and Heimer, 1986; Nitecka and Frotscher, 1989; Muller et al., 2011), although the types of postsynaptic receptors associated with these inputs were not identified. Likewise, there is electrophysiological evidence for muscarinic activation of BLa interneurons, but the receptor subtypes were not determined (Washburn and Moises, 1992; Yajeya et al., 1997).

Excitatory and inhibitory axon terminals express M1R-ir

M1R-ir was seen in axon terminals forming asymmetrical synapses or symmetrical synapses, but the former greatly outnumbered the latter. M1R-ir in both types of terminals was often concentrated along the presynaptic membrane at the active zone of the synapse, suggesting that acetylcholine regulates neurotransmitter release at these sites via M1Rs. Most M1R+ terminals forming asymmetrical synapses contacted dendritic spines, the great majority of which were also M1R+. M1R+ terminals forming symmetrical synapses mainly contacted M1R+ perikarya, axon initial segments, and small-caliber dendritic shafts. Unlike the presynaptic axon terminals, M1R-ir in the postsynaptic targets of these terminals was not concentrated at the synapse. The ubiquitous presence of M1R-ir in these postsynaptic structures suggests that most belong to pyramidal cells (see above), and the postsynaptic targets of terminals forming asymmetrical synapses (dendritic spines) or symmetrical synapses (perikarya, axon initial segments, and small-caliber dendritic shafts) is consistent with the organization of inputs to BLa pyramidal cells (Muller et al., 2006).

Previous electron microscopic studies of the basolateral amygdala indicate that axon terminals forming asymmetrical synapses represent glutamatergic inputs from the cerebral cortex (Hall, 1972; Smith and Paré, 1994; Brinley-Reed et al., 1995; Farb and LeDoux, 1999; Smith et al., 2000), midline/intralaminar thalamus (Carlsen and Heimer, 1988; LeDoux et al., 1991), and internuclear and intranuclear amygdalar connections arising from basolateral amygdalar pyramidal neurons (Stefanacci et al., 1992; Smith and Paré, 1994; Paré et al., 1995; Smith et al., 2000). Many of the symmetrical synapses onto BLa pyramidal cells are formed by several distinct subpopulations of GABAergic interneurons (Carlsen, 1988; Aylward and Totterdell, 1993; Smith et al., 2000; McDonald et al., 2002; Muller et al., 2003, 2006, 2007). However, monoaminergic projections from the brainstem (Asan, 1998, Muller et al., 2007, 2009; Farb and LeDoux, 2010) and cholinergic projections from the basal forebrain (Carlsen and Heimer, 1986; Muller et al., 2011) also form symmetrical synapses. The use of a dual-labeling immunoperoxidase technique to study M1/VAChT localization in the present investigation did not allow us to examine possible M1R-ir in VAChT+ cholinergic terminals. To the authors' knowledge there have been no studies that have examined whether amygdalopetal BF cholinergic neurons express M1R mRNA or protein.

In the present study, and in a previous study (Muller et al., 2011), we found that cholinergic terminals were often in close proximity to non-cholinergic terminals forming symmetrical and asymmetrical synapses onto BLa pyramidal neurons. Recent re-examination of light microscopic preparations from the previous study revealed that VAChT+ terminals were usually about 1–3 μm apart (see Fig. 1B of Muller et al., 2011). Likewise, electron microscopic observations in the previous study (see Figs. 3 and 4 of Muller et al., 2011) and the present study (Fig. 9) found that VAChT+ terminals were sometimes 1–2 μm apart (although most appeared further apart in single thin sections due to the extreme thinness of these sections [60–70 nm]). Thus, because of the very high density of VAChT+ terminals in the BLa, the great majority of non-cholinergic M1R+ terminals are probably within 1–2 μm of a cholinergic terminal. The short distance between cholinergic terminals and M1R+ terminals suggests that synaptic spillover of acetylcholine during high rates or bursts of cholinergic activity, or possible diffusion from non-synaptic cholinergic terminals, could modulate the release of glutamate or GABA from neighboring M1R+ terminals (Vizi and Kiss, 1998, 2010; Sarter et al., 2009). For comparison, it has been suggested that in the striatum and substantia nigra the sphere of influence of released dopamine is about 2 μm for activation of low-affinity dopamine receptors and 7–8 μm for high-affinity receptors (Rice and Cragg, 2008).

The anatomical findings of the present study are consistent with electrophysiological studies of the BLa that have demonstrated modulation of glutamate and GABA release from axon terminals by muscarinic cholinergic mechanisms. Thus, Washburn and Moises (1992) reported that muscarinic agonists produced reductions in the amplitude of synaptically-evoked EPSPs and IPSPs in pyramidal cells of the BLa via a presynaptic mechanism, although the subtype of muscarinic receptor was not determined. Yajeya and coworkers used pirenzepine to block M1Rs and estimated that approximately 20% of the reduction in the amplitude of synaptically-evoked EPSPs in BLa pyramidal cells was mediated by presynaptic M1Rs (Yajeya et al., 2000). Recent studies in our lab indicate that acetylcholine

suppresses both cortical and thalamic inputs to BLa pyramidal cells via presynaptic M1Rs (Liu et al., 2012). Sugita et al. (1991) determined that presynaptic M1Rs were also responsible for inhibiting synaptically-evoked release of GABA onto pyramidal cells of the lateral amygdalar nucleus.

Some of the M1R+ terminals forming symmetrical synapses were very large and had numerous synaptic vesicles and mitochondrial profiles, characteristic of the distinctive type 1 axon terminals of GABAergic basal forebrain (BF) afferents to the BLa (McDonald et al., 2011). These BF GABAergic projection neurons are intermingled with cholinergic neurons of the BF, but constitute only about 10–15% of BF amydalopetal neurons (Mascagni and McDonald, 2009). BF type 1 axons synapse with both pyramidal cells and parvalbumin-containing interneurons in the BLa (McDonald et al., 2011). Likewise, M1R+ type 1 axons observed in the present study appeared to synapse with both presumptive pyramidal cells and interneurons, identified on the basis of their distinctive morphological features. Since presynaptic muscarinic receptors generally inhibit neurotransmitter release, the expression of M1R-ir in these type 1 BF terminals suggests that phasic release of acetylcholine by BF cholinergic axons might be followed by a rapid attenuation of GABA release from type 1 BF axons. This postulated coordinated action of BF cholinergic and GABAergic axons may play an important role in regulating oscillatory activity in the BLa, as in the hippocampus (Freund and Buzsaki, 1996; Borhegyi et al., 2004).

Cholinergic axon terminals form synapses with M1R+ structures

This is the first investigation to use serial section reconstructions to study the synaptic incidence of cholinergic terminals in the BLa. This analysis revealed that about three-quarters (76%) of VAChT+ cholinergic axon terminals form synapses. Since an unfavorable orientation may hinder the identification of synapses, especially the symmetrical synapses formed by cholinergic terminals, it seems likely that an even higher percentage of cholinergic terminals in the BLa may actually form synapses. These data corroborate and extend previous non-quantitative ultrastructural studies of cholinergic terminals in the BLa using ChAT (Wainer et al., 1984; Carlsen and Heimer, 1986; Nitecka and Frotscher, 1989; Houser, 1990; Li et al., 2001) or VAChT (Muller et al., 2011) as cholinergic markers, in which it was reported that most cholinergic terminals formed synapses. In the present investigation the main postsynaptic targets of cholinergic axons were small-caliber dendritic shafts (41%; all of which were M1R+) and spines (50%; 86% of which were M1R+). These percentages are very similar to those obtained in a previous study of VAChT+ inputs to CaMK+ (i.e., pyramidal cell) small-caliber dendritic shafts (40%) and spines (40%) (Muller et al., 2011).

Only some of the synapses formed by VAChT+ terminals onto M1R+ postsynaptic structures exhibited M1R-ir along the postsynaptic membrane. It was not uncommon, however, to see particulate M1R-ir along the plasma membrane outside of the active zone of VAChT+ synapses in V-VIP preparations. This label may represent perisynaptic M1Rs that are activated by acetylcholine that reaches these receptors via spillover from nearby cholinergic terminals forming synapses, similar to what is seen with other metabotropic receptors (Vizi et al., 2010). The finding of M1R-ir in the great majority of dendritic spines

that are postsynaptic to cholinergic terminals suggests that these spines are directly modulated by acetylcholine released at the synapse.

The release of acetylcholine at synapses with pyramidal cell distal dendrites and associated spines should not only be able to activate M1Rs expressed by these postsynaptic structures, but also, via spillover from these synapses, be able to activate M1Rs in neighboring spines that do not receive cholinergic inputs. Because of the very high density of VAChT+ terminals in the BLa, it is also likely that spillover from synaptic VAChT+ terminals could activate M1Rs in non-cholinergic axon terminals forming asymmetrical glutamatergic synapses and symmetrical GABAergic synapses with the distal dendritic domain of pyramidal cells (see above). The presynaptic M1R-mediated inhibition of GABA release (Sugita et al., 1991) at inhibitory synapses with pyramidal cells should contribute to the increased excitability of these cells produced by the postsynaptic effects of acetylcholine (Washburn and Moises, 1992, Womble and Moises, 1992, 1993). M1R-mediated effects at spines of pyramidal cells, the main targets of excitatory input (Muller et al., 2006), are probably more complex since activation of M1Rs in spines should be mainly depolarizing, but activation of presynaptic M1Rs in excitatory terminals synapsing with these spines should inhibit glutamate release from these terminals, thereby reducing excitation (Yajeya et al., 2000, Liu et al., 2012).

The expression of M1R in a subset of spines suggests that M1R-mediated effects may be associated with specific excitatory inputs to these spines from particular cortical, thalamic, or intra-amygdalar sources. One possible function of this M1R modulation of excitatory inputs to pyramidal cells is to affect synaptic plasticity involved in mnemonic processes. Thus, colocalization of M1R with the N-methyl-D-aspartate receptor (NMDAR) is seen in dendritic spines of hippocampal pyramidal cells, where activation of M1Rs potentiate NMDAR currents (Marino et al., 1998). Since NMDARs are associated with induction of long-term potentiation (LTP) in the hippocampus, it is not surprising that activation of M1Rs enhances LTP (Shinoe et al., 2005). Like the hippocampus, spines in BLa pyramidal cells contain NMDA receptors (Farb et al., 1995; Gracy and Pickel, 1995), which suggests that M1R in these spines may potentiate NMDAR currents, which are known to play an important role in the acquisition of fear conditioning (Maren and Fanselow, 1995; Blair et al., 2001; Rodrigues et al., 2004; Sigurdsson et al., 2007). It remains to be determined if these interactions involving M1Rs and NMDARs are involved in the muscarinic enhancement of fear conditioning consolidation (Vazdarjanova and McGaugh, 1999).

Comparison with the cerebral cortex

Because the cell types in the BLa are cortex-like (McDonald 1992a); Carlsen and Heimer, 1988), it is of interest to compare M1R localization and its association with cholinergic terminals in the BLa with that seen in the neocortex and hippocampus. One major similarity of M1R localization in the rodent BLa (McDonald and Mascagni, 2010; present study), neocortex (Yamasaki et al., 2010), and hippocampus (Rouse et al., 1998; Yamasaki et al., 2010) is its predominance in pyramidal cells. As in the BLa, only a subset of pyramidal cell spines in the hippocampus were M1R+ (Rouse et al., 1998), although the percentages of M1R+ spines in the BLa (ca. 60%) were higher than that seen in the hippocampus (ca. 40%).

Similar to our study of the rat BLa, a recent study of the mouse neocortex and hippocampus did not report accumulations of M1R-ir in dendritic regions subjacent to cholinergic terminal contacts (Yamasaki et al., 2010), suggesting that acetylcholine in both regions may reach most M1Rs via diffusion through the extracellular space. However, unlike the BLa, very few cholinergic terminals in the mouse neocortex and hippocampus appear to make synaptic contacts (Yamasaki et al., 2010). It remains to be determined if M1R has a similar localization pattern in the various cortical areas in other species where a much higher synaptic incidence has been reported (e.g., rat parietal cortex [Turrini et al., 2001] and human temporal cortex [Smiley et al., 1997]).

Previous studies of M1R localization in a variety of cortical areas in the primate and rodent cortex have reported a paucity of M1R+ axon terminals (Mrzljak et al., 1993; Rouse et al., 1998; Disney et al., 2006; Yamasaki et al., 2010). These results contrast sharply with our finding that M1R+ terminals are common in the BLa. As mentioned above, our results are consistent with electrophysiological studies which have reported M1R modulation of transmitter release in the BLa. However, since M1R modulation of transmitter release has also been described in the cortex (Kremin et al., 2006; Hasselmo and Bower, 1992), it is surprising that more M1R terminals were not seen in immunohistochemical studies of cortical regions. This may be, in part, a technical issue. Previous cortical studies employed immunogold-silver or non-intensifed DAB immunoperoxidase techniques. We used nickel-enhanced DAB and V-VIP immunoperoxidase techniques. It is well established that the non-intensifed DAB immunoperoxidase method is more sensitive than immunogold-silver, and that nickel-intensified DAB is more sensitive than both of these techniques (Sesack, 2006; Hancock, 1986). We have found that immunoperoxidase using the V-VIP chromogen is also more sensitive than non-intensified DAB (personal observations of AJM and JFM). It remains to be determined, however, if the use of the latter techniques would result in a larger percentage of M1R+ terminals in cortical structures.

Acknowledgments

Grant Sponsor: National Institutes of Health Grant R01-DA027305.

Role of authors:

Study concept and design: JFM, AJM

Acquisition of data: JFM, AJM, FM, VZ

Analysis and interpretation of data: JFM, AJM

Drafting of the manuscript: JFM, AJM

Obtained funding: AJM

Study supervision: AJM

LITERATURE CITED

Amaral DG, Bassett JL. Cholinergic innervation of the monkey amygdala: an immunohistochemical analysis with antisera to choline acetyltransferase. J Comp Neurol. 1989; 281:337–361. [PubMed: 2703552]

Asan E. The catecholaminergic innervation of the rat amygdala. Adv Anat Embryol Cell Biol. 1998; 142:1–118. [PubMed: 9586282]

Aylward RL, Totterdell S. Neurons in the ventral subiculum, amygdala and entorhinal cortex which project to the nucleus accumbens: their input from somatostatin-immunoreactive boutons. J Chem Neuroanat. 1993; 6:31–42. [PubMed: 7679909]

Ben-Ari Y, Zigmond RE, Shutter CC, Lewis PR. Regional distribution of choline acetyltransferase and acetylcholinesterase within the amygdaloid complex and stria terminalis system. Brain Res. 1977; 120:435–444. [PubMed: 832133]

Blair HT, Schafe GE, Bauer EP, Rodrigues SM, LeDoux JE. Synaptic plasticity in the lateral amygdala: a cellular hypothesis of fear conditioning. Learn Mem. 2001; 8:229–242. [PubMed: 11584069]

Bonner TI, Buckley NJ, Young AC, Brann MR. Identification of a family of muscarinic acetylcholine receptor genes. Science. 1987; 237:527–532. [PubMed: 3037705]

Borhegyi Z, Varga V, Szilágyi N, Fabo D, Freund TF. Phase segregation of medial septal GABAergic neurons during hippocampal theta activity. J Neurosci. 2004; 24:8470–8479. [PubMed: 15456820]

Brinley-Reed M, Mascagni F, McDonald AJ. Synaptology of prefrontal cortical projections to the basolateral amygdala: an electron microscopic study in the rat. Neurosci Lett. 1995; 202:45–48. [PubMed: 8787827]

Buckley NJ, Bonner TI, Brann MR. Localization of a family of muscarinic receptor mRNAs in rat brain. J Neurosci. 1988; 8:4646–4652. 1988. [PubMed: 3199198]

Carlsen J, Zaborszky L, Heimer L. Cholinergic projections from the basal forebrain to the basolateral amygdaloid complex: a combined retrograde fluorescent and immunohistochemical study. J. Comp. Neurol. 1985; 234:155–167. [PubMed: 3886715]

Carlsen J. Immunocytochemical localization of glutamate decarboxylase in the rat basolateral amygdaloid nucleus, with special reference to GABAergic innervation of amygdalostriatal projection neurons. J Comp Neurol. 1988; 273:513–526. [PubMed: 3062049]

Carlsen J, Heimer L. A correlated light and electron microscopic immunocytochemical study of cholinergic terminals and neurons in the rat amygdaloid body with special emphasis on the basolateral amygdaloid nucleus. J Comp Neurol. 1986; 244:121–136. [PubMed: 3512630]

Carlsen J, Heimer L. The basolateral amygdaloid complex as a cortical-like structure. Brain Res. 1988; 441:377–380. [PubMed: 2451985]

Disney AA, Domakonda KV, Aoki C. Differential expression of muscarinic acetylcholine receptors across excitatory and inhibitory cells in visual cortical areas V1 and V2 of the macaque monkey. J Comp Neurol. 2006; 499:49–63. [PubMed: 16958109]

Ehlert, FJ.; Roeske, WR.; Yamamura, HI. Molecular biology, pharmacology, and brain distribution of subtypes of the muscarinic receptor. In: Bloom, FE.; Kupfer, DJ., editors. Psychopharmacology: the Fourth Generation of Progress. New York: Raven Press; 1995. p. 111-124.

Farb CR, Aoki C, Ledoux JE. Differential localization of NMDA and AMPA receptor subunits in the lateral and basal nuclei of the amygdala: a light and electron microscopic study. J Comp Neurol. 1995; 362:86–108. [PubMed: 8576430]

Farb CR, Ledoux JE. Afferents from rat temporal cortex synapse on lateral amygdala neurons that express NMDA and AMPA receptors. Synapse. 1999; 33:218–229. [PubMed: 10420169]

Farb CR, Chang W, Ledoux JE. Ultrastructural characterization of noradrenergic axons and Beta-adrenergic receptors in the lateral nucleus of the amygdala. Front Behav Neurosci. 2010; 4:162. [PubMed: 21048893]

Freund TF, Buzsáki G. Interneurons of the hippocampus. Hippocampus. 1996; 6:347–470. [PubMed: 8915675]

Gilmor ML, Nash NR, Roghani A, Edwards RH, Yi H, Hersch SM, Levey AI. Expression of the putative vesicular acetylcholine transporter in rat brain and localization in cholinergic synaptic vesicles. J. Neurosci. 1996; 16:2179–2190. [PubMed: 8601799]

Girgis M. Acetylcholinesterase enzyme localization in the amygdala: a comparative histochemical and ultrastructural study. Acta Anat. (Basel). 1980; 106:192–202. [PubMed: 6770574]

Gracy KN, Pickel VM. Comparative ultrastructural localization of the NMDAR1 glutamate receptor in the rat basolateral amygdala and bed nucleus of the stria terminalis. J Comp Neurol. 1995; 362:71–85. [PubMed: 8576429]

Hall E. The amygdala of the cat: a Golgi study. Z Zellforsch. 1972; 134:439–458. [PubMed: 4638299]

Hancock MB. Two color immunoperoxidase staining: visualization of anatomic relationships between immunoreactive neural elements. Am J Anat. 1986; 175:343–352. [PubMed: 2422916]

Hasselmo ME, Bower JM. Cholinergic suppression specific to intrinsic not afferent fiber synapses in rat piriform (olfactory) cortex. J Neurophysiol. 1992; 67:1222–1229. [PubMed: 1597708]

Hellendall RP, Godfrey DA, Ross CD, Armstrong DM, Price JL. The distribution of choline acetyltransferase in the rat amygdaloid complex and adjacent cortical areas, as determined by quantitative micro-assay and immunohistochemistry. J Comp Neurol. 1986; 249:486–498. [PubMed: 2427553]

Houser CR. Cholinergic synapses in the central nervous system: studies of the immunocytochemical localization of choline acetyltransferase. J Electron Microsc Tech. 1990; 15:2–19. [PubMed: 2187067]

Koliatsos VE, Martin LJ, Walker LC, Richardson RT, DeLong MR, Price DL. Topographic, non-collateralized basal forebrain projections to amygdala, hippocampus, and anterior cingulate cortex in the rhesus monkey. Brain Res. 1988; 463:133–139. [PubMed: 3196902]

Kordower JH, Bartus RT, Marciano FF, Gash DM. Telencephalic cholinergic system of the New World monkey (Cebus apella): morphological and cytoarchitectonic assessment and analysis of the projection to the amygdala. J Comp Neurol. 1989; 279:528–545. [PubMed: 2465322]

Kremin T, Gerber D, Giocomo LM, Huang SY, Tonegawa S, Hasselmo ME. Muscarinic suppression in stratum radiatum of CA1 shows dependence on presynaptic M1 receptors and is not dependent on effects at GABA(B) receptors. Neurobiol Learn Mem. 2006; 85:153–163. [PubMed: 16290192]

LeDoux JE, Farb CR, Milner TA. Ultrastructure and synaptic associations of auditory thalamo-amygdala projections in the rat. Exp Brain Res. 1991; 85:577–586. [PubMed: 1717305]

Levey AI, Kitt CA, Simonds WF, Price DL, Brann MR. Identification and localization of muscarinic acetylcholine receptor proteins in brain with subtype-specific antibodies. J Neurosci. 1991; 11:3218–3226. [PubMed: 1941081]

Li R, Nishijo H, Wang Q, Uwano T, Tamura R, Ohtani O, Ono T. Light and electron microscopic study of cholinergic and noradrenergic elements in the basolateral nucleus of the rat amygdala: evidence for interactions between the two systems. J Comp Neurol. 2001; 439:411–425. [PubMed: 11596063]

Liu, L.; McDonald, AJ.; Mott, DD. Neuroscience Meeting Planner. New Orleans, LA: Society for Neuroscience; 2012. Muscarinic modulation of glutamatergic neurotransmission in the basolateral amygdala. Program No. 143.06. 2012. 2012 Online

Maren S, Fanselow MS. Synaptic plasticity in the basolateral amygdala induced by hippocampal formation stimulation in vivo. J Neurosci. 1995; 15:7548–7564. [PubMed: 7472506]

Marino MJ, Rouse ST, Levey AI, Potter LT, Conn PJ. Activation of the genetically defined m1 muscarinic receptor potentiates N-methyl-D-aspartate (NMDA) receptor currents in hippocampal pyramidal cells. Proc Natl Acad Sci U S A. 1998; 95:11465–11470. [PubMed: 9736760]

Mascagni F, McDonald AJ. Parvalbumin-immunoreactive neurons and GABAergic neurons of the basal forebrain project to the rat basolateral amygdala. Neuroscience. 2009; 160:805–812. [PubMed: 19285116]

McDonald, AJ. Cell types and intrinsic connections of the amygdala. In: Aggleton, JP., editor. The Amygdala. New York: Wiley-Liss; 1992a. p. 67-96.

McDonald AJ. Projection neurons of the basolateral amygdala: a correlative Golgi and retrograde tract tracing study. Brain Res Bull. 1992b; 28:179–185. [PubMed: 1375860]

McDonald AJ, Muller JF, Mascagni F. GABAergic Innervation of alpha type II calcium/calmodulin-dependent protein kinase immunoreactive pyramidal neurons in the rat basolateral amygdala. J. CompNeurol. 2002; 446:199–218.

McDonald AJ, Mascagni F. Neuronal localization of m1 muscarinic receptor immunoreactivity in the rat basolateral amygdala. Brain Struct Funct. 2010; 215:37–48. [PubMed: 20503057]

McDonald AJ, Muller JF, Mascagni F. Postsynaptic targets of GABAergic basal forebrain projections to the basolateral amygdala. Neuroscience. 2011; 183:144–159. [PubMed: 21435381]

McGaugh JL. The amygdala modulates the consolidation of memories of emotionally arousing experiences. Annu Rev Neurosci. 2004; 27:1–28. [PubMed: 15217324]

Mesulam MM, Mufson EJ, Wainer BH, Levey AI. Central cholinergic pathways in the rat: an overview based on an alternative nomenclature (Ch1–Ch6). Neuroscience. 1983a; 10:1185–1201. [PubMed: 6320048]

Mesulam MM, Mufson EJ, Levey AI, Wainer BH. Cholinergic innervation of cortex by the basal forebrain: cytochemistry and cortical connections of the septal area, diagonal band nuclei, nucleus basalis (substantia innominata), and hypothalamus in the rhesus monkey. J Comp Neurol. 1983b; 214:170–197. [PubMed: 6841683]

Mrzljak L, Levey AI, Goldman-Rakic PS. Association of m1 and m2 muscarinic receptor proteins with asymmetric synapses in the primate cerebral cortex: morphological evidence for cholinergic modulation of excitatory neurotransmission. Proc Natl Acad Sci U S A. 1993; 90:5194–5198. [PubMed: 8389473]

Muller JF, Mascagni F, McDonald AJ. Synaptic connections of distinct interneuronal subpopulations in the rat basolateral amygdalar nucleus. J Comp Neurol. 2003; 456:217–236. [PubMed: 12528187]

Muller JF, Mascagni F, McDonald AJ. Pyramidal cells of the rat basolateral amygdala: synaptology and innervation by parvalbumin-immunoreactive interneurons. J Comp Neurol. 2006; 494:635–650. [PubMed: 16374802]

Muller JF, Mascagni F, McDonald AJ. Postsynaptic targets of somatostatin-containing interneurons in the rat basolateral amygdala. J. Comp. Neurol. 2007; 500:513–529. [PubMed: 17120289]

Muller JF, Mascagni F, McDonald AJ. Cholinergic innervation of pyramidal cells and interneurons in the rat basolateral amygdala. J. Comp. Neurol. 2011; 519:790–805. [PubMed: 21246555]

Nitecka L, Frotscher M. Organization and synaptic interconnections of GABAergic and cholinergic elements in the rat amygdaloid nuclei: single and double immunolabeling studies. J Comp Neurol. 1989; 279:470–488. [PubMed: 2918082]

Paré D, Smith Y, Paré JF. Intra-amygdaloid projections of the basolateral and basomedial nuclei in the cat: Phaseolus vulgaris-leucoagglutinin anterograde tracing at the light and electron microscopic level. Neuroscience. 1995; 69:567–583. [PubMed: 8552250]

Paxinos, G.; Watson, C. The Rat Brain in Stereotaxic Coordinates. New York: Academic Press; 1997.

Peters, A.; Palay, SL.; Webster, HD. The fine structure of the nervous system. New York: Oxford University Press; 1991.

Power AE, Vazdarjanova A, McGaugh JL. Muscarinic cholinergic influences in memory consolidation. Neurobiol Learn Mem. 2003a; 80:178–193. [PubMed: 14521862]

Power AE, McIntyre CK, Litmanovich A, McGaugh JL. Cholinergic modulation of memory in the basolateral amygdala involves activation of both m1 and m2 receptors. Behav Pharmacol. 2003b; 14:207–213. [PubMed: 12799522]

Power JM, Sah P. Competition between calcium-activated K+ channels determines cholinergic action on firing properties of basolateral amygdala projection neurons. J Neurosci. 2008; 28:3209–3220. [PubMed: 18354024]

Rao ZR, Shiosaka S, Tohyama M. Origin of cholinergic fibers in the basolateral nucleus of the amygdaloid complex by using sensitive double-labeling technique of retrograde biotinized tracer and immunocytochemistry. J Hirnforsch. 1987; 28:553–560. [PubMed: 3320200]

Rice ME, Cragg SJ. Dopamine spillover after quantal release: rethinking dopamine transmission in the nigrostriatal pathway. Brain Res Rev. 2008; 58:303–313. [PubMed: 18433875]

Rodrigues SM, Schafe GE, LeDoux JE. Molecular mechanisms underlying emotional learning and memory in the lateral amygdala. Neuron. 2004; 44:75–91. [PubMed: 15450161]

Rouse ST, Gilmor ML, Levey AI. Differential presynaptic and postsynaptic expression of m1-m4 muscarinic acetylcholine receptors at the perforant pathway/granule cell synapse. Neuroscience. 1998; 86:221–232. [PubMed: 9692756]

Richelson, E. Cholinergic transduction. In: Bloom, FE.; Kupfer, DJ., editors. Psychopharmacology: the Fourth Generation of Progress. New York: Raven Press; 1995. p. 125-134.

Sarter M, Parikh V, Howe WM. Phasic acetylcholine release and the volume transmission hypothesis: time to move on. Nat Rev Neurosci. 2009; 10:383–390. [PubMed: 19377503]

Sesack, SR.; Miner, LH.; Omelchenko, N. Preembedding immunoelectron microscopy: applications for studies of the nervous system. In: Zaborsky, L.; Wouterlood, FG.; Lanciego, JL., editors. Neuroanatomical Tract-Tracing 3. New York: Springer; 2006. p. 6-71.

Shinoe T, Matsui M, Taketo MM, Manabe T. Modulation of synaptic plasticity by physiological activation of M1 muscarinic acetylcholine receptors in the mouse hippocampus. J Neurosci. 2005; 25:11194–11200. [PubMed: 16319319]

Sigurdsson T, Doyère V, Cain CK, LeDoux JE. Long-term potentiation in the amygdala: a cellular mechanism of fear learning and memory. Neuropharmacology. 2007; 52:215–227. [PubMed: 16919687]

Smiley JF, Morrell F, Mesulam MM. Cholinergic synapses in human cerebral cortex: an ultrastructural study in serial sections. Exp Neurol. 1997; 144:361–368. [PubMed: 9168836]

Smith Y, Paré D. Intra-amygdaloid projections of the lateral nucleus in the cat: PHA-L anterograde labeling combined with postembedding GABA and glutamate immunocytochemistry. J Comp Neurol. 1994; 342:232–248. [PubMed: 7911130]

Smith Y, Paré J-F, Paré D. Differential innervation of parvalbumin-immunoreactive interneurons of the basolateral amygdaloid complex by cortical and intrinsic inputs. J Comp Neurol. 2000; 416:496–508. [PubMed: 10660880]

Stefanacci L, Farb CR, Pitkänen A, Go G, LeDoux JE, Amaral DG. Projections from the lateral nucleus to the basal nucleus of the amygdala: a light and electron microscopic PHA-L study in the rat. J Comp Neurol. 1992; 323:586–601. [PubMed: 1430325]

Sugita S, Uchimura N, Jiang ZG, North RA. Distinct muscarinic receptors inhibit release of gamma-aminobutyric acid and excitatory amino acids in mammalian brain. Proc Natl Acad Sci U S A. 1991; 88:2608–2611. [PubMed: 1672454]

Svendsen CN, Bird ED. Acetylcholinesterase staining of the human amygdala. Neurosci Lett. 1985; 54:313–318. [PubMed: 3991070]

Turrini P, Casu MA, Wong TP, De Koninck Y, Ribeiro-da-Silva A, Cuello AC. Cholinergic nerve terminals establish classical synapses in the rat cerebral cortex: synaptic pattern and age-related atrophy. Neuroscience. 2001; 105:277–285. [PubMed: 11672595]

Van Haeften T, Wouterlood FG. Neuroanatomical tracing at high resolution. J Neurosci Methods. 2000; 103:107–116. [PubMed: 11074100]

Vazdarjanova A, McGaugh JL. Basolateral amygdala is involved in modulating consolidation of memory for classical fear conditioning. J Neurosci. 1999; 19:6615–6622. 1999. [PubMed: 10414989]

Vizi ES, Kiss JP. Neurochemistry and pharmacology of the major hippocampal transmitter systems: synaptic and nonsynaptic interactions. Hippocampus. 1998; 8:566–607. [PubMed: 9882017]

Vizi ES, Fekete A, Karoly R, Mike A. Non-synaptic receptors and transporters involved in brain functions and targets of drug treatment. Br J Pharmacol. 2010; 160:785–809. [PubMed: 20136842]

Wainer BH, Bolam JP, Freund TF, Henderson Z, Totterdell S, Smith AD. Cholinergic synapses in the rat brain: a correlated light and electron microscopic immunohistochemical study employing a monoclonal antibody against choline acetyltransferase. Brain Res. 1984; 308:69–76. [PubMed: 6478204]

Washburn MS, Moises HC. Muscarinic responses of rat basolateral amygdaloid neurons recorded in vitro. J Physiol. 1992; 449:121–154. [PubMed: 1522506]

Weihe E, Tao-Cheng JH, Schäfer MK, Erickson JD, Eiden LE. Visualization of the vesicular acetylcholine transporter in cholinergic nerve terminals and its targeting to a specific population of small synaptic vesicles. Proc Natl Acad Sci U S A. 1996; 93:3547–5352. [PubMed: 8622973]

Womble MD, Moises HC. Muscarinic inhibition of M-current and a potassium leak conductance in neurones of the rat basolateral amygdala. J Physiol. 1992; 457:93–114. [PubMed: 1338469]

Womble MD, Moises HC. Muscarinic modulation of conductances underlying the afterhyperpolarization in neurons of the rat basolateral amygdala. Brain Res. 1993; 621:87–96. [PubMed: 8221077]

Woolf NJ, Eckenstein F, Butcher LL. Cholinergic systems in the rat brain: I. Projections to the limbic telencephalon. Brain Res Bull. 1984; 13:751–784. [PubMed: 6532518]

Yajeya J, de la Fuente Juan A, Merchan MA, Riolobos AS, Heredia M, Criado JM. Cholinergic responses of morphologically and electrophysiologically characterized neurons of the basolateral complex in rat amygdala slices. Neuroscience. 1997; 78:731–743. [PubMed: 9153654]

Yajeya J, De La Fuente A, Criado JM, Bajo V, Sánchez-Riolobos A, Heredia M. Muscarinic agonist carbachol depresses excitatory synaptic transmission in the rat basolateral amygdala in vitro. Synapse. 2000; 38:151–160. [PubMed: 11018789]

Yamasaki M, Matsui M, Watanabe M. Preferential localization of muscarinic M1 receptor on dendritic shaft and spine of cortical pyramidal cells and its anatomical evidence for volume transmission. J Neurosci. 2010; 30:4408–4418. [PubMed: 20335477]

Záborszky L, Heimer L, Eckenstein F, Leranth C. GABAergic input to cholinergic forebrain neurons: an ultrastructural study using retrograde tracing of HRP and double immunolabeling. J Comp Neurol. 1986; 250:282–295. [PubMed: 3528237]

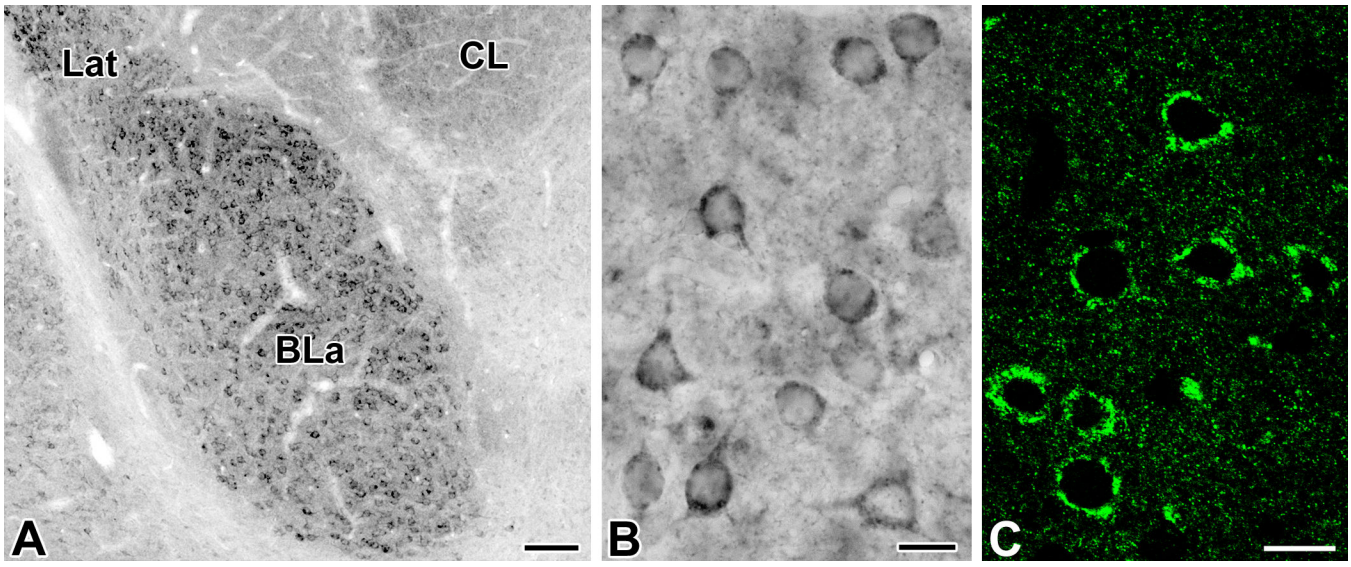

Figure 1.

M1R-ir in the BLa at the light microscopic level. **A:** Low-power photomicrograph of the dorsolateral corner of the amygdala showing robust M1R-ir in the BLa (immunoperoxidase technique with nickel intensification of DAB). Note that perikaryal M1R-ir is much stronger in the BLa and lateral nucleus (Lat) than in the lateral subdivision of the central nucleus (CL). **B:** Higher-power photomicrograph of M1R-ir in the BLa (immunoperoxidase technique with nickel intensification of DAB). Note strong perikaryal staining in pyramidal cells and significant punctuate neuropilar staining. **C:** High-power photomicrograph of M1R-ir in the BLa (immunofluorescence technique). The punctate neuropilar label between pyramidal cell perikarya is more easily seen using immunofluorescence. Scale bars = A: 100 μm; B and C: 20 μm.

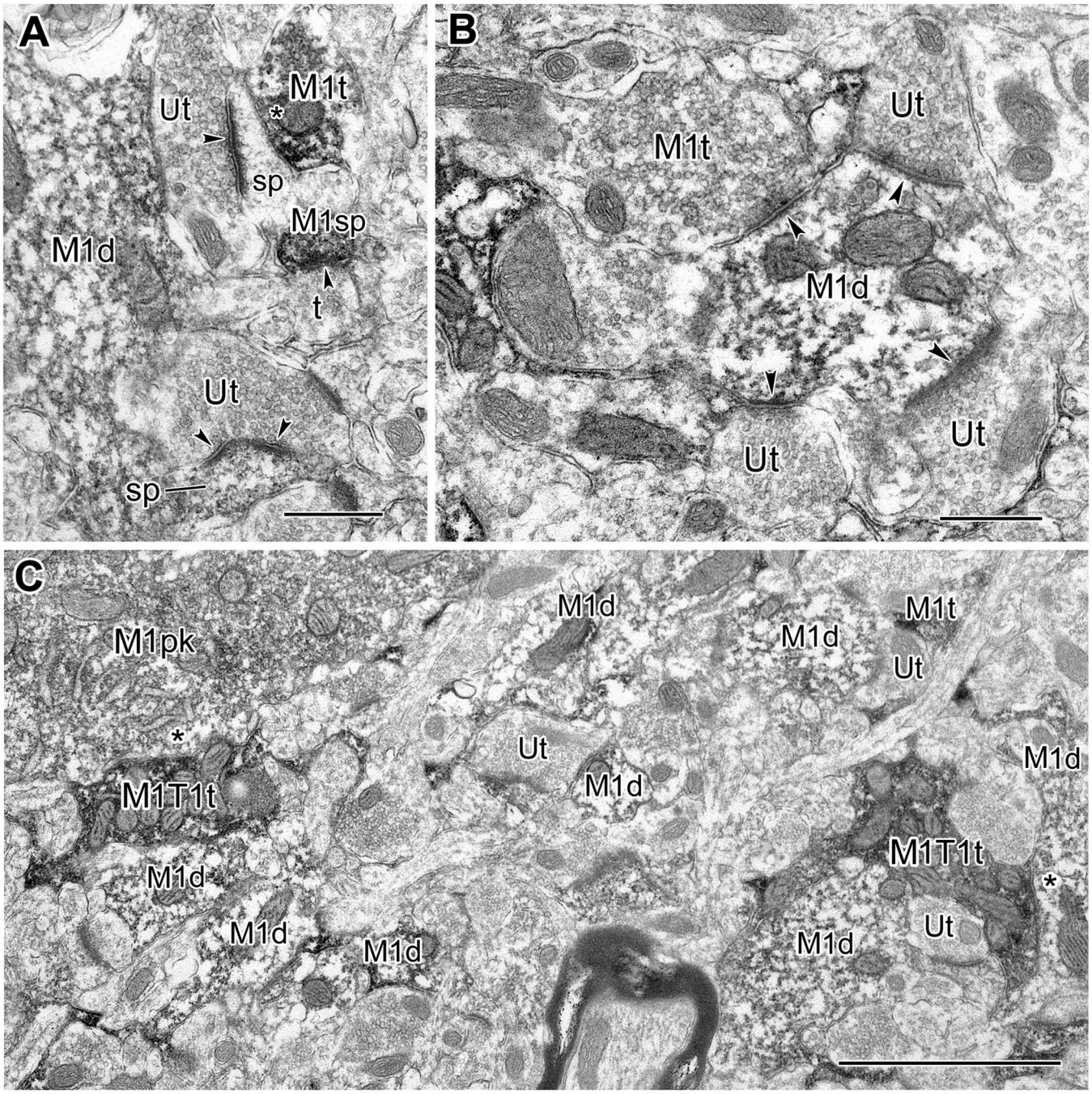

Fig. 2.

M1R-ir in the BLa at the electron microscopic level in tissue stained using nickel-enhanced DAB as a chromogen. **A:** An unlabeled spine (sp, top) receives asymmetrical synaptic contact from an unlabeled terminal (Ut, arrowhead), and a symmetrical synaptic contact from an M1R+ terminal (M1t, asterisk). An M1R+ spine (M1sp) receives an asymmetrical synapse from an unlabeled terminal (t, arrowhead). An M1R+ dendrite (M1d) gives rise to a spine (sp, bottom) that receives asymmetrical synaptic contact from an adjacent unlabeled terminal (Ut, arrowheads). **B:** An M1R+ dendrite (M1d) receives asymmetrical synaptic

contacts (arrowheads) from a lightly immunoreactive terminal (M1t) and three unlabeled terminals (Ut). This synaptic configuration involving multiple excitatory inputs is typical of interneuronal dendrites (Muller et al., 2011). **C:** Two large M1R+ axon terminals whose morphology resembles that of type 1 terminals formed by GABAergic afferents from the basal forebrain (M1T1t) are strongly M1R+. The M1T1t on the left makes symmetrical synaptic contact with an M1R+ perikaryon (M1pk, asterisk), and the M1T1t on the right makes symmetrical synaptic contact with an M1R+ dendrite (M1d, asterisk). The M1R+ perikaryon had a large pyramidal-shaped soma, and received only symmetrical synaptic inputs, typical of pyramidal cells (Muller et al., 2006). In serial sections, the M1T1t on the left and right were found to make synaptic contacts onto the other adjacent M1R+ dendrites (M1d). Additional M1R+ dendrites (M1d), an M1R+ terminal (M1t, upper right), and several unlabeled terminals (Ut) in the field are also indicated. Scale bars = 0.5 μm in A, B; 2 μm in C.

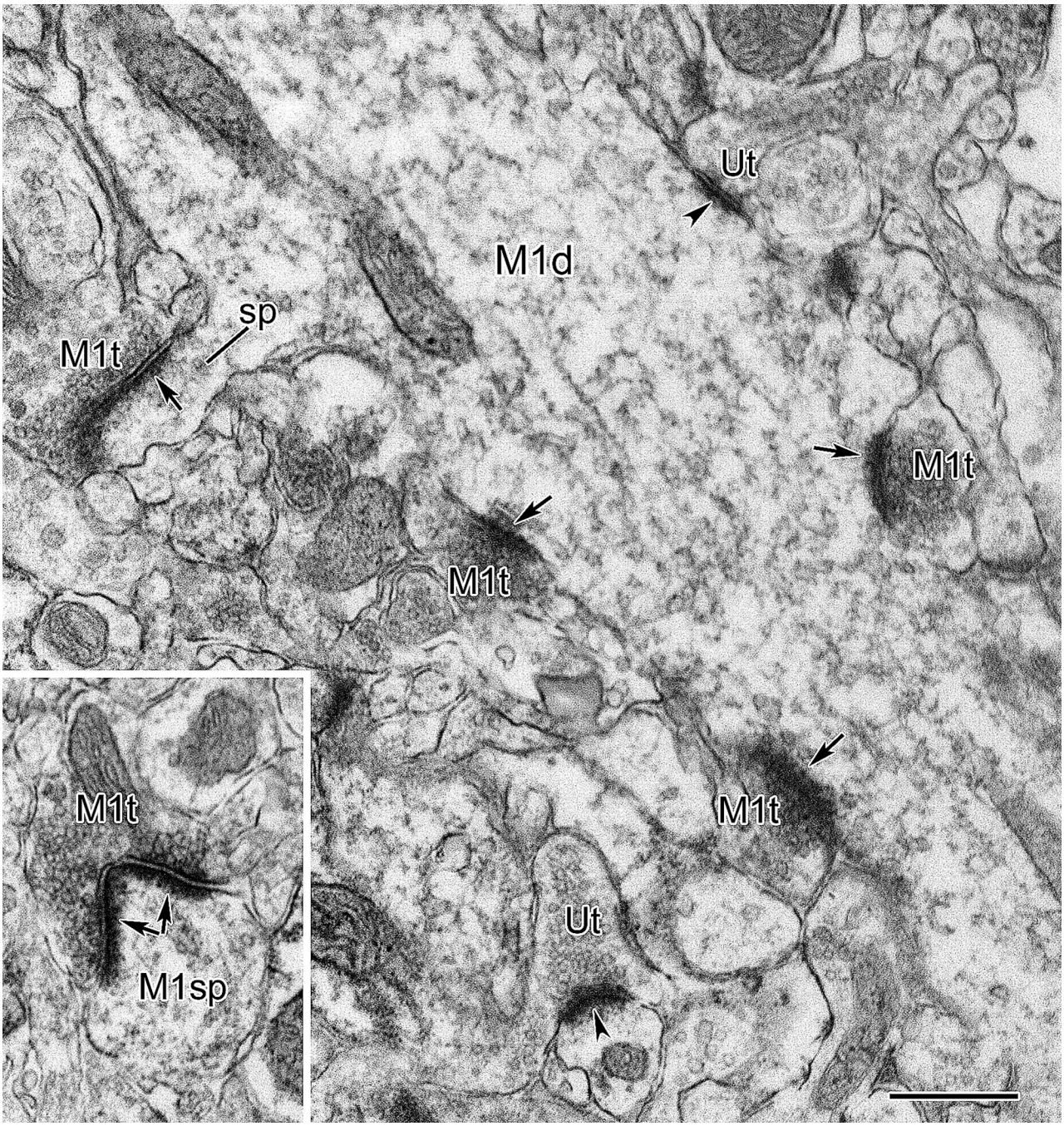

Fig. 3.

Electron micrograph of a large-caliber M1R+ dendrite in a Ni-DAB preparation. Flocculent reaction product decorates the microtubules of this dendrite (M1d), and light immunoreactivity is also seen in its spine (sp). The spine receives an asymmetrical synapse (arrow) from an M1R+ terminal (M1t). The dendritic shaft receives asymmetrical synaptic contacts from 3 M1R+ terminals (M1t, arrows), and an unlabeled terminal (Ut, arrowhead). Another unlabeled terminal (Ut; bottom) makes asymmetrical contact with a small dendrite

(arrowhead). Inset: A nearby M1R+ spine (M1sp) receives an asymmetrical synaptic contact from an M1R+ terminal (M1t, arrows. Scale = 0.5 μm.

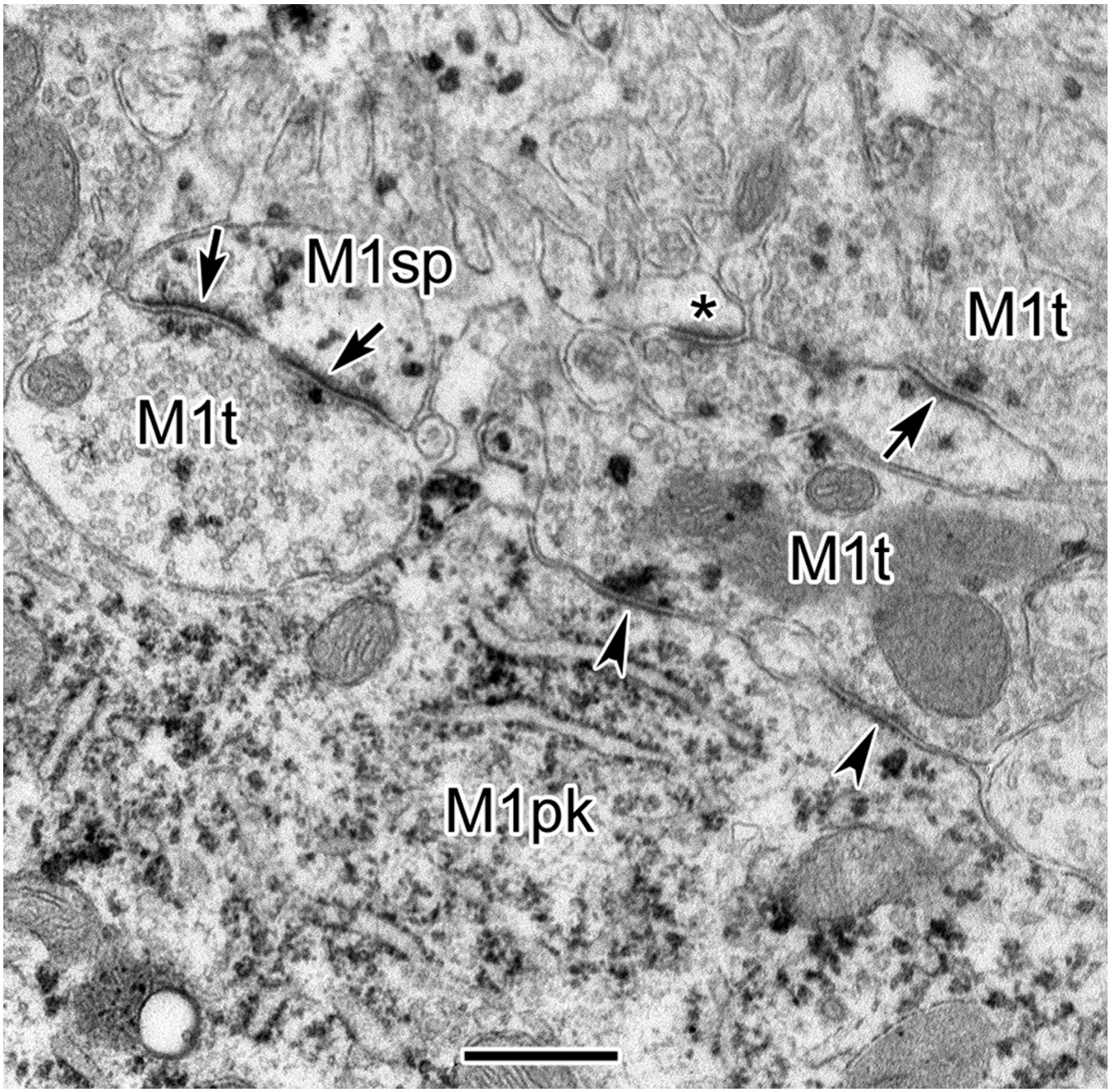

Fig. 4.

Electron micrograph of M1R-ir in the BLa in tissue stained using V-VIP as a chromogen. An M1R+ perikaryon (M1pk) receives two symmetrical synaptic contacts from an M1R+ terminal (M1t, middle, right, arrowheads). An M1R+ spine (M1sp) receives asymmetrical synaptic contacts from an M1R+ terminal (M1t, left, arrows). Two other examples of M1R+ spines receiving asymmetrical synaptic contacts from M1R+ terminals are also indicated in the upper right. The arrow shows a synapse formed by an M1R+ terminal (M1t) with a spine containing particulate M1R reaction product. The asterisk indicates an unlabeled spine receiving an asymmetrical synaptic contact from an M1R+ terminal (M1t). Note the location

of the particulate M1R reaction product along the presynaptic membrane of some of these M1R+ terminals. Scale bar = 0.5 μm.

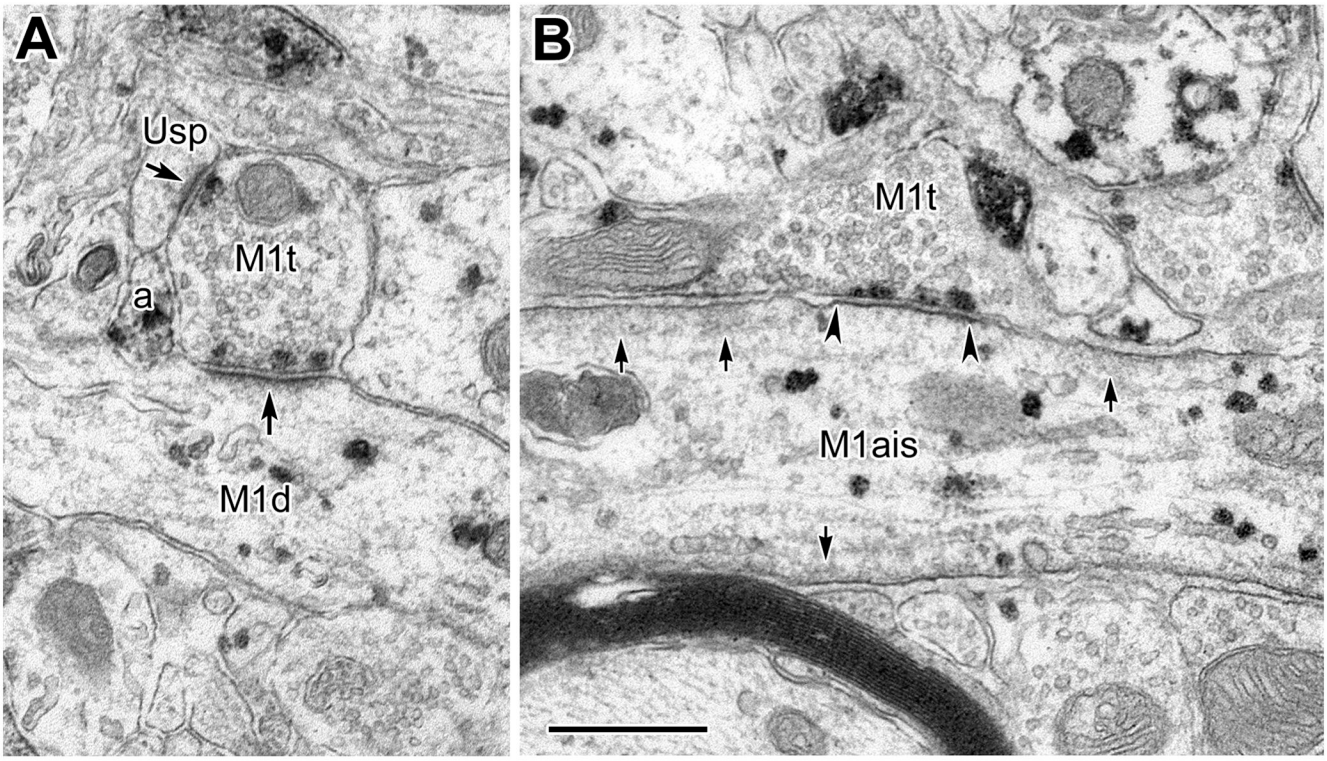

Fig. 5.

A: An M1R+ terminal (M1t) makes an asymmetrical synaptic contact onto an M1R+ dendrite (M1d, arrow) and an unlabeled spine (Usp, arrow). An adjacent M1R+ astrocytic profile is also indicated (a). **B:** An M1R+ axon initial segment (M1ais) receives symmetrical synaptic contact from an M1R+ terminal (M1t, arrowheads). The dense membrane undercoating, typical of axon initial segments, is indicated with small arrows. Note the location of the particulate M1R reaction product along the presynaptic membrane of both of these M1R+ terminals. Scale bar = 0.5 μm (for A, B).

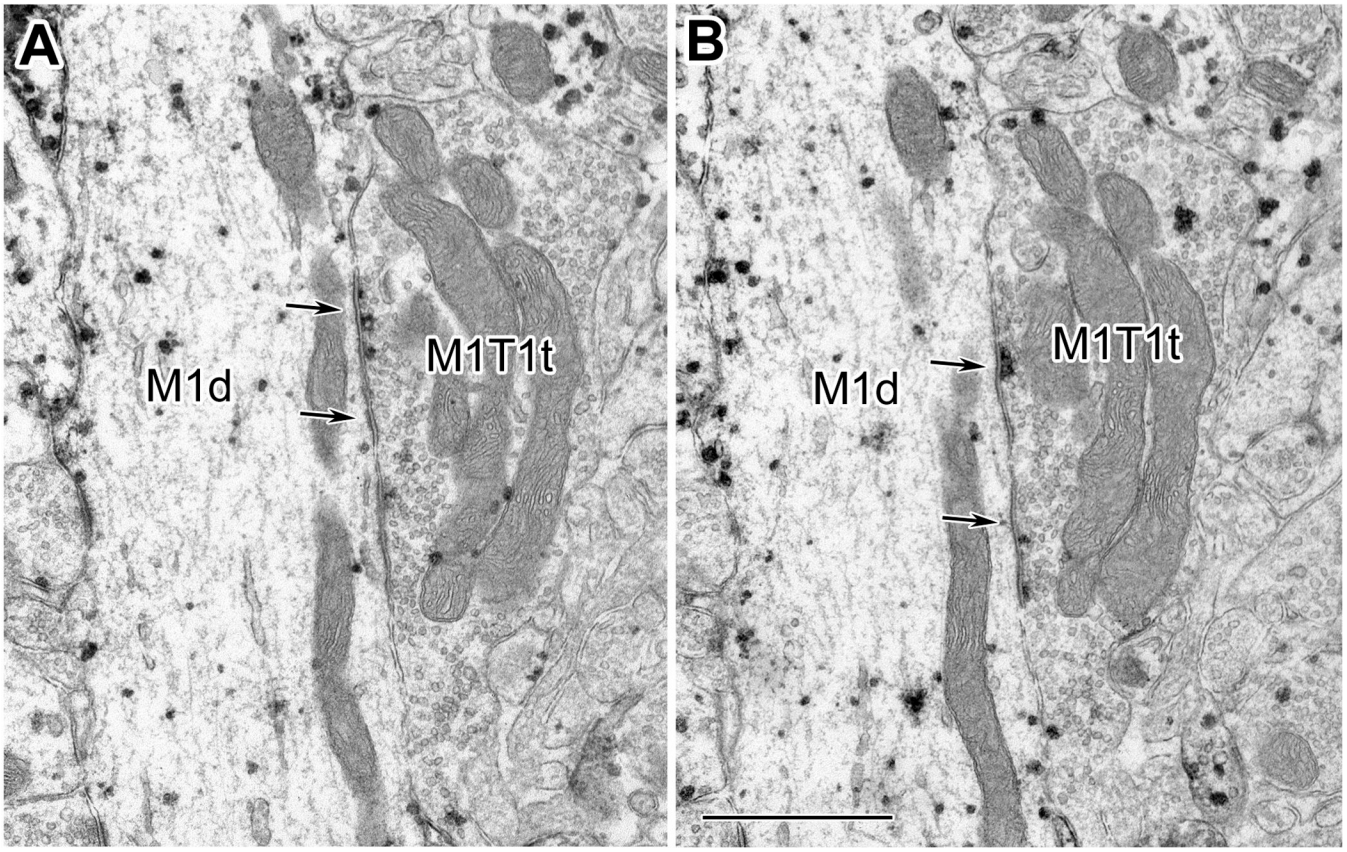

Fig. 6.

A, B: Serial electron micrographs of a large M1R+ terminal (M1T1t) that exhibits the distinctive morphology exhibited by type 1 GABAergic terminals from the basal forebrain (McDonald et al., 2011) making symmetrical synaptic contact (arrows) with an M1R+ dendrite (M1d). This dendrite was free of spines and had numerous excitatory inputs, suggesting that it was interneuronal (Muller et al., 2011). Note the location of the particulate M1R reaction product along the presynaptic membrane of this M1R+ terminal. In addition, a VAChT+ terminal was seen, in serial sections, less than one micron deep to those pictured, adjacent to both the lower edge of the M1T1t and M1d. Scale bar = 0.5 μm (for A, B).

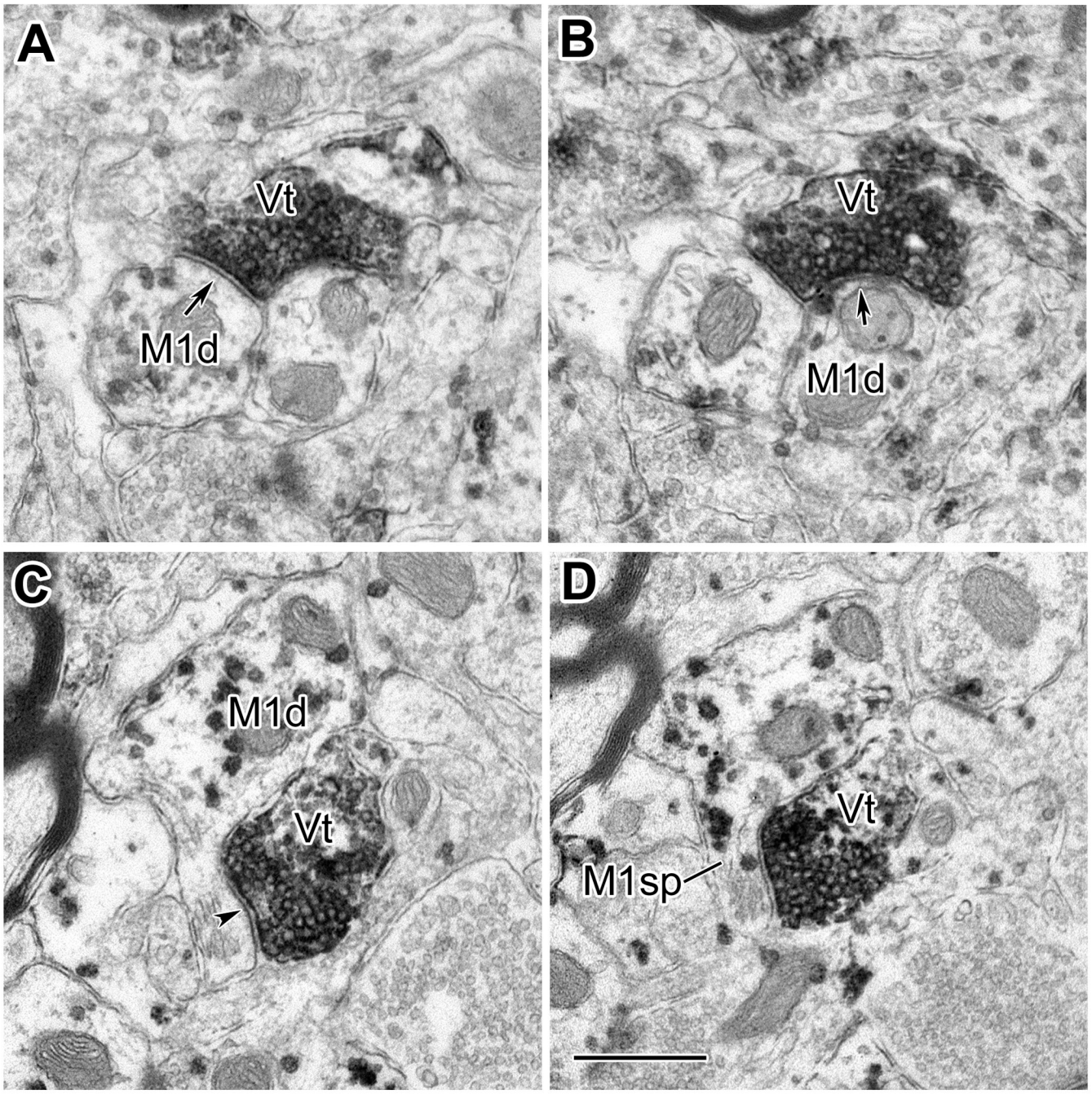

Fig. 7.

A, B: Serial electron micrographs of a VAChT+ terminal (Vt) making synaptic contacts onto two neighboring dendrites (M1d, arrows). **C, D:** Serial electron micrographs of a spine emerging from an M1R+ dendrite (M1d) that receives symmetrical synaptic input from a VAChT+ terminal (Vt, arrowhead). In panel D it is apparent that the spine is M1R+ (M1sp). Scale bar = 0.5 μm (for A–D).

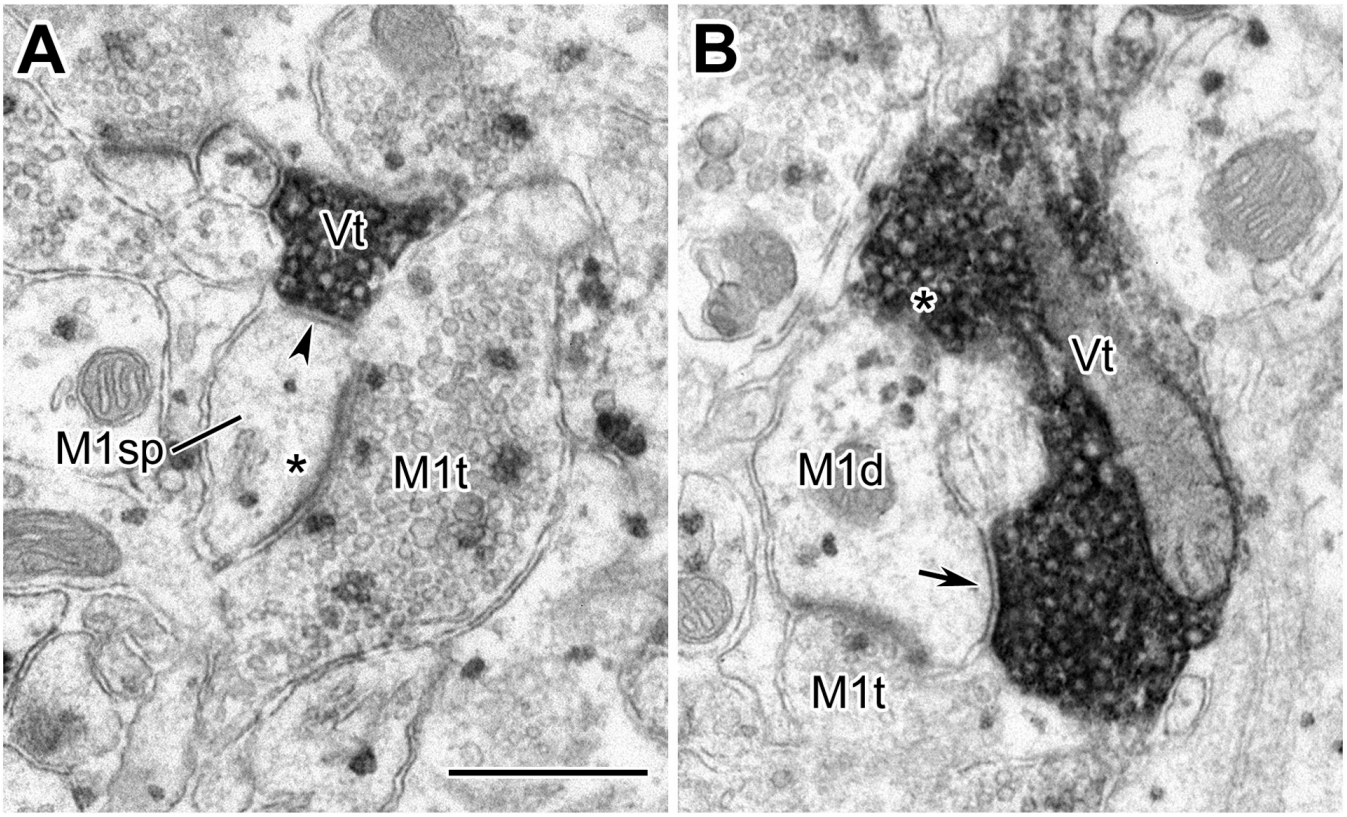

Fig. 8.

A: An M1R+ spine (M1sp) receives a symmetrical synaptic contact from a VAChT+ terminal (Vt, arrowhead), and an asymmetrical synapse from an M1R+ terminal (M1t, asterisk). **B:** A VAChT+ axon (Vt) makes synaptic contacts at two locations with an M1R+ small- caliber dendrite (M1d, arrow, asterisk), and a M1R+ terminal (M1t) forms an asymmetrical synapse with the same spine. Scale bar = 0.5 μm (for A, B).

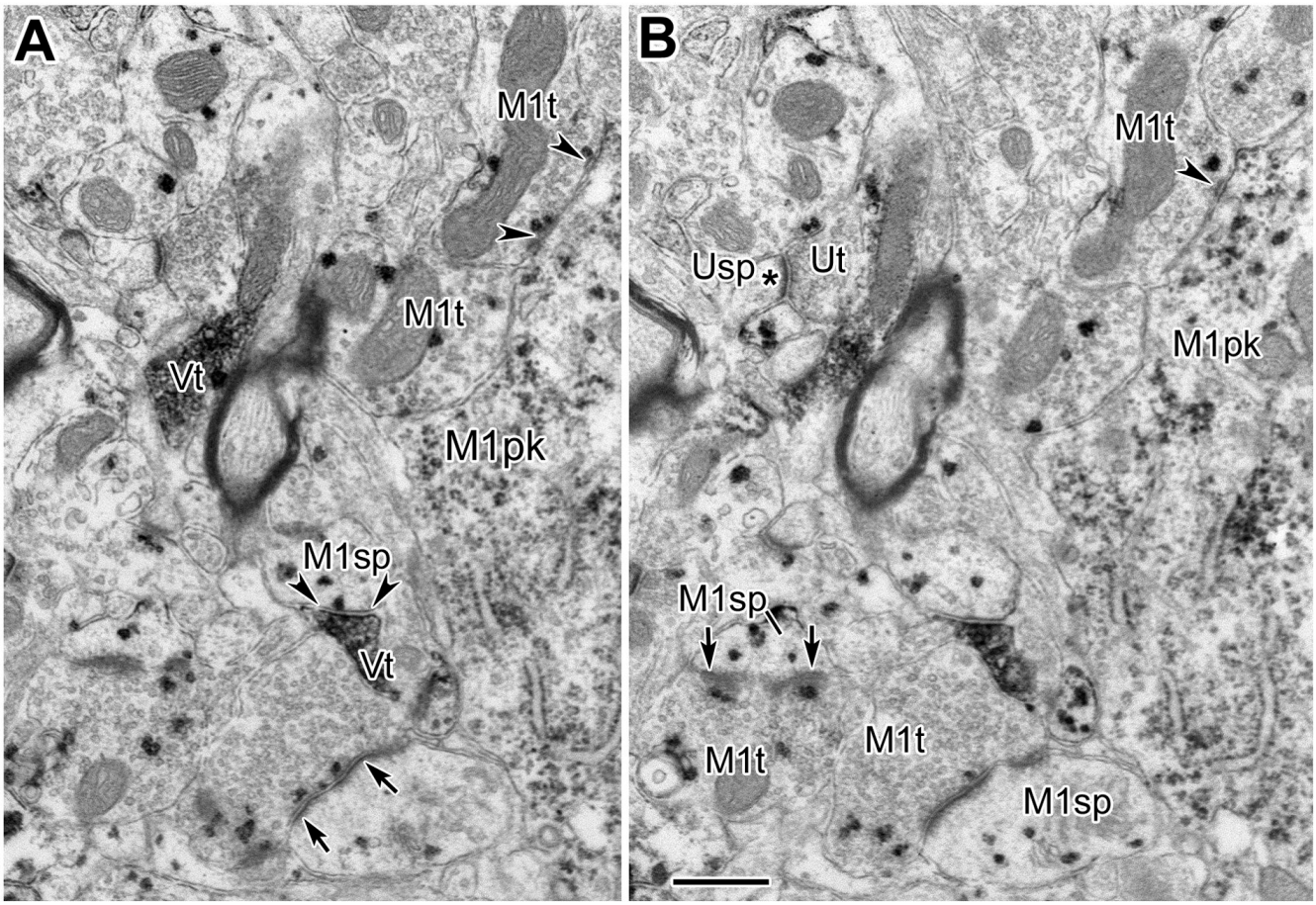

Fig. 9.

A, B: Serial electron micrographs from a VAChT/M1R dual labeled preparation. A VAChT + terminal (Vt, lower middle) forms a symmetrical synapse with an M1R+ spine (M1sp, arrowheads in A). Another VAChT terminal is also seen in this field (Vt, left). Two M1R+ spines (M1sp, bottom left, right in B) receive asymmetrical synaptic contacts from M1R+ terminals (M1t, arrows). An M1R+ perikaryon (M1pk, right) receives punctate symmetrical contacts from an M1R+ terminal (M1t, upper right, arrowheads). An unlabeled terminal making asymmetrical synaptic contact with an unlabeled spine is also indicated (Ut, Usp, asterisk). Scale bar = 0.5 μm (for A, B).

Table 1

Table of Primary Antibodies

Antigen	Immunogen	Manufacturer	Dilution Used
m1 muscarinic acetylcholine receptor	Purified GST fusion protein of a part of the third intracellular loop (amino acid residues 227–353) of the human m1 muscarinic acetylcholine receptor	Sigma Chemical Co. (St. Louis), rabbit polyclonal, #M-9808	1:250–400
Vesicular acetylcholine transporter	Synthetic carboxy-terminal 20 amino acid sequence (511–530) of the cloned rat vesicular acetylcholine transporter	ImmunoStar (Hudson, WI), goat polyclonal, #24286	1:4000

Table 2

Postsynaptic targets of M1R+ axon terminals forming asymmetrical synapses, and the percentage of each target that was M1R+.

Chromogen	Brain	Perikaryon	Large Dendrite	Small Dendrite	Spine
Ni-DAB	EM 91	3/62 (4.8%) 100% M1R+	6/62 (9.7%) 100% M1R+	13/62 (21.0%) 100% M1R+	40/62 (64.5%) 85% M1R+
	EM 95	0/74 (0%)	10/74 (13.5%) 100% M1R+	15/74 (20.3%) 80% M1R+	49/74 (66.2%) 83.7% M1R+
	Total	3/136 (2.2%) 100% M1R+	16/136 (11.8%) 100% M1R+	28/136 (20.6%) 89.3% M1R+	89/136 (65.4%) 84.3% M1R+
V-VIP	EM 108	0/41 (0%)	3/41 (7.3%) 100% M1R+	7/41 (17.1%) 100% M1R+	31/41 (75.6%) 87.1% M1R+
	EM 109	0/83 (0%)	0/83 (0%)	12/83 (14.5%) 100% M1R+	71/83 (85.6%) 93.0% M1R+
	Total	0/124 (0%)	3/124 (2.4%) 100% M1R+	19/124 (15.3%) 100% M1R+	102/124 (82.3%) 91.2% M1R+
	Combined Total	3/260 (1.2%) 100% M1R+	19/260 (7.3%) 100% M1R+	47/260 (18.1%) 93.6% M1R+	191/260 (73.5%) 88.0% M1R+

Table 3

Postsynaptic targets of M1R+ axon terminals forming symmetrical synapses, and the percentage of each target that was M1R+.

Chromogen	Brain	Perikaryon or AIS [1]	Large Dendrite	Small Dendrite	Spine
Ni-DAB	EM 91	5/7 (71.4%) 100% M1R+	1/7 (14.3%) 100% M1R+	0/7 (0%)	1/7 (14.3%) 0% M1R+
	EM 95	2/8 (25.0%) 100% M1R+	2/8 (25.0%) 100% M1R+	4/8 (50.0%) 100% M1R+	0/8 (0%)
	Total	7/15 (46.7%) 100% M1R+	3/15 (20.0%) 100% M1R+	4/15 (26.7%) 100% M1R+	1/15 (6.7%) 0% M1R+
V-VIP	EM 108	5/13 (38.5%) 100% M1R+	1/13 (7.7%) 100% M1R+	6/13 (46.2%) 100% M1R+	1/13 (7.7%) 0% M1R+
	EM 109	7/20 (35.0%) 100% M1R+	0/20 (0%)	10/20 (50.0%) 100% M1R+	3/20 (15.0%) 100% M1R+
	Total	12/33 (36.4%) 100% M1R+	1/33 (3.0%) 100% M1R+	16/33 (48.5%) 100% M1R+	4/33 (12.1%) 75.0% M1R+
	Combined Total	19/48 (39.6%) 100% M1R+	4/48 (8.3%) 100% M1R+	20/48 (41.7%) 100% M1R+	5/48 (10.4%) 60.0% M1R+

[1] AIS: axon initial segment

Table 4

Postsynaptic targets of cholinergic VAChT+ axon terminals and the percentage of each target that was M1R+.

Brain	Perikaryon	Large Dendrite	Small Dendrite	Spine
EM 109	2 (4.3%) 100% M1R+	0 (0%)	17 (37.0%) 100% M1R+	27 (58.7%) 81.5% M1R+
EM 108	1 (1.9%) 100% M1R+	5 (9.4%) 100% M1R+	24 (45.3%) 100% M1R+	23 (43.4%) 91.3% M1R+
Total	3 (3.0%) 100% M1R+	5 (5.1%) 100% M1R+	41 (41.4%) 100% M1R+	50 (50.5%) 86.0% M1R+